

**Global approach to top-quark flavor-changing interactions**Gauthier Durieux,<sup>1,2</sup> Fabio Maltoni,<sup>2</sup> and Cen Zhang<sup>3</sup><sup>1</sup>*Laboratory for Elementary Particle Physics, Cornell University, Ithaca, New York 14853, USA*<sup>2</sup>*Centre for Cosmology, Particle Physics and Phenomenology, Université catholique de Louvain, B-1348 Louvain-la-Neuve, Belgium*<sup>3</sup>*Department of Physics, Brookhaven National Laboratory, Upton, New York 11973, USA*

(Received 28 January 2015; published 9 April 2015)

We adopt a fully gauge-invariant effective-field-theory approach for parametrizing top-quark flavor-changing-neutral-current interactions. It allows for a global interpretation of experimental constraints (or measurements) and the systematic treatment of higher-order quantum corrections. We discuss some recent results obtained at next-to-leading-order accuracy in QCD and perform, at that order, a first global analysis of a subset of the available experimental limits in terms of effective operator coefficients. We encourage experimental collaborations to adopt this approach and extend the analysis by using all information they have prime access to.

DOI: [10.1103/PhysRevD.91.074017](https://doi.org/10.1103/PhysRevD.91.074017)

PACS numbers: 14.65.Ha, 12.60.-i, 11.30.Hv, 12.38.Bx

**I. INTRODUCTION**

The wealth of top quarks produced at the LHC has moved top physics to a precision era. Detailed information on the top couplings, their strengths as well as Lorentz structures, has been collected and possible deviations are being constrained. In addition, interactions that are absent or suppressed in the standard model (SM) become more and more accessible. Among these, top-quark flavor-changing-neutral-current interactions (FCNCs) play a special role. Highly suppressed by the Glashow-Iliopoulos-Maiani mechanism, the SM predicts them to be negligible. Branching ratios for top FCNC decays are notably of the order of  $10^{-12}$ – $10^{-15}$  [1–3] in the SM. Any evidence for such processes would thus immediately point to new physics. In addition, the recent discovery of a scalar particle closely resembling the SM Higgs boson [4,5] has made Higgs-mediated FCNCs experimentally searchable.

A wide variety of limits have been set on top-quark FCNC interactions, see, e.g., Ref. [6]. Single-top  $p\bar{p} \rightarrow t$  production has been searched at the Tevatron by CDF [7] and at the LHC by ATLAS [8,9] while D0 [10,11] and CMS [12] considered the  $p\bar{p} \rightarrow tj$  production mode. In addition, CMS also searched for single-top production in association with a photon [13] or a charged lepton pair [14]. At LEP2,  $e^+e^- \rightarrow tj$  has been investigated by all four groups [15–20] while, at HERA, the single-top  $e^-p \rightarrow e^-t$  production has been considered by ZEUS [21,22] and H1 [23–25]. The FCNC decay processes  $t \rightarrow j\ell^+\ell^-$  and  $t \rightarrow j\gamma$  have also been studied, at the Tevatron by CDF [26–28] and D0 [29], and at the LHC by ATLAS [30–32] and CMS [33,34]. Finally,  $t \rightarrow jh$  has been constrained by CMS [35] that combined the leptonic  $WW^*$ ,  $\tau\tau$ ,  $ZZ^*$  and  $\gamma\gamma$  channels while ATLAS used the last (and most sensitive) one only [36,37].

The effective field theory (EFT) [38–40] is a particularly relevant framework for parametrizing new physics

and has been used in many top-quark FCNC studies [41–56]. It does not only incorporate all possible effects of new heavy physics in a model-independent way, but also orders them and allows us to consistently take into account higher-order quantum corrections. Leading-order (LO) predictions are actually insufficient when an accurate interpretation of observables in terms of theory parameters is aimed at. QCD corrections in top-decay processes [57–62] typically amount to approximately 10%, while they can reach between 30% and 80% in production processes [63–67]. The running and mixing of operator coefficients should also be taken into account. While an EFT description in principle requires a complete basis of operators to be used, neglecting some of them may appear consistent when only lowest-order estimates of specific processes are considered. The next-to-leading-order (NLO) counterterms as well as the renormalization-group (RG) running and mixings of operator coefficients however clearly reveal the unnatural and inconsistent character of neglecting some operators. A proper EFT description of new physics should necessarily be global. Currently, however, the limits obtained by experimental collaborations almost always assume one single FCNC interaction is present at the time.

The aim of this paper is to outline a general strategy for studying top-quark interactions in the context of an EFT, starting from the case of top-quark FCNC processes. Our main points can be summarized as follows:

- (i) The widely used formalism that relies on dimension-four and -five operators in the electroweak (EW) broken phase is inadequate in several respects.
- (ii) Calculations of FCNC processes can now be performed (in most cases already automatically) in the EFT framework at NLO in QCD. Some new NLO results for four-fermion operator contributions are provided here for the first time.

- (iii) A consistent analysis should be global, i.e., consider all operators contributing to a given process. For such an approach to be successful a sufficiently large (and complete) set of observables should be identified. We show that for FCNC interactions involving the top quark this is already close to being possible with the current measurements and suggest a minimal set of observables accessible at the LHC to complete the set.

The paper is organized as follows. Section III discusses the operator mixing effects at NLO in QCD and demonstrates the need for a global approach. We show some NLO results for single-top production processes in Sec. IV, including both two- and four-fermion operators. A first global analysis incorporating the most sensitive experimental searches is finally carried out in Sec. V.

## II. EFFECTIVE FIELD THEORY

Let us start, in this Sec. II, by presenting the effective operators relevant for a NLO description of top-quark FCNC processes, and highlighting the insufficiencies of the dimension-four and -five operators formalism.

### A. Fully gauge-invariant operators

Assuming the full standard model  $SU(3)_C \times SU(2)_L \times U(1)_Y$  gauge symmetry as well as baryon and lepton number conservations,<sup>1</sup> the first beyond-the-standard-model operators  $O_i$  constructed with standard-model fields only arise at dimension six. Restricting our EFT description to this level, the Lagrangian can be written [69]

$$\mathcal{L}_{\text{EFT}} = \mathcal{L}_{\text{SM}} + \sum_i \frac{C_i}{\Lambda^2} O_i, \quad (1)$$

where  $C_i$ 's are dimensionless coefficients and  $\Lambda$  is a mass scale. We will use the operator basis and notations of Ref. [70], which includes 59 independent dimension-six operators. Our choice of operator normalization follows Ref. [62].

Amongst the ones contributing (up to NLO in QCD) to top-quark FCNC processes, different categories can be distinguished. We first consider operators involving exactly two quarks. Their Lorentz structures can be used to separate three subclasses: vector, scalar, and tensor operators. Omitting indices for clarity (notably flavor ones) and denoting the fermionic flavor-generic gauge eigenstates by  $q, u, d, l$  and  $e$ , they are

$$\begin{aligned} O_{\varphi q}^1 &\equiv \frac{y_i^2}{2} \bar{q} \gamma^\mu q \varphi^\dagger i \overleftrightarrow{D}_\mu \varphi, \\ O_{\varphi q}^3 &\equiv \frac{y_i^2}{2} \bar{q} \gamma^\mu \tau^I q \varphi^\dagger i \overleftrightarrow{D}_\mu^I \varphi, \\ O_{\varphi u} &\equiv \frac{y_i^2}{2} \bar{u} \gamma^\mu u \varphi^\dagger i \overleftrightarrow{D}_\mu \varphi, \\ O_{u\varphi} &\equiv -y_i^3 \bar{q} u \tilde{\varphi} \quad (\varphi^\dagger \varphi - v^2/2), \\ O_{uB} &\equiv y_i g_Y \bar{q} \sigma^{\mu\nu} u \tilde{\varphi} B_{\mu\nu}, \\ O_{uW} &\equiv y_i g_W \bar{q} \sigma^{\mu\nu} \tau^I u \tilde{\varphi} W_{\mu\nu}^I, \\ O_{uG} &\equiv y_i g_s \bar{q} \sigma^{\mu\nu} T^A u \tilde{\varphi} G_{\mu\nu}^A, \end{aligned}$$

with  $\overleftrightarrow{D}_\mu^{(I)} \equiv (\tau^I) \overrightarrow{D}_\mu - \overleftarrow{D}_\mu (\tau^I)$  and  $\tilde{\varphi} \equiv i\tau^2 \varphi^* \equiv \varepsilon \varphi^*$ . Out of the  $O_{\varphi q}^\pm \equiv O_{\varphi q}^1 \pm O_{\varphi q}^3$  operators, only  $O_{\varphi q}^-$  contributes to FCNC processes in the up sector. We note that the vector contributions to the  $tqZ$  vertices arising from  $O_{\varphi q}^-$  and  $O_{\varphi u}$ , and the tensor ones arising from  $O_{uB}$  and  $O_{uW}$  have not been both simultaneously considered in experimental searches so far. Next we consider operators involving two quarks and two leptons:

$$\begin{aligned} O_{lq}^1 &\equiv \bar{l} \gamma_\mu l \bar{q} \gamma^\mu q, \\ O_{lq}^3 &\equiv \bar{l} \gamma_\mu \tau^I l \bar{q} \gamma^\mu \tau^I q, \\ O_{lu} &\equiv \bar{l} \gamma_\mu l \bar{u} \gamma^\mu u, \\ O_{eq} &\equiv \bar{e} \gamma^\mu e \bar{q} \gamma_\mu q, \\ O_{eu} &\equiv \bar{e} \gamma_\mu e \bar{u} \gamma^\mu u, \\ O_{lequ}^1 &\equiv \bar{l} e \varepsilon \bar{q} u, \\ O_{lequ}^3 &\equiv \bar{l} \sigma_{\mu\nu} e \varepsilon \bar{q} \sigma^{\mu\nu} u. \end{aligned}$$

It is useful to introduce the  $O_{lq}^\pm \equiv O_{lq}^1 \pm O_{lq}^3$  combinations.  $O_{lq}^-$  contains the interactions of two up-type quarks with two charged leptons (or, of two down-type quarks with two neutrinos) while  $O_{lq}^+$  notably gives rise to interactions between two up-type quarks and two neutrinos (or, two down-type quarks and two charged leptons). Finally, there are four-quark operators. The complete basis has been discussed in Ref. [71]. Here we use the basis of Ref. [70] in which there are no tensor operators:

$$\begin{aligned} O_{qq}^1 &\equiv \bar{q} \gamma_\mu q \bar{q} \gamma^\mu q, & O_{qq}^3 &\equiv \bar{q} \gamma_\mu \tau^I q \bar{q} \gamma^\mu \tau^I q, \\ O_{qu}^1 &\equiv \bar{q} \gamma_\mu q \bar{u} \gamma^\mu u, & O_{qu}^8 &\equiv \bar{q} \gamma_\mu T^A q \bar{u} \gamma^\mu T^A u, \\ O_{qd}^1 &\equiv \bar{q} \gamma_\mu q \bar{d} \gamma^\mu d, & O_{qd}^8 &\equiv \bar{q} \gamma_\mu T^A q \bar{d} \gamma^\mu T^A d, \\ O_{uu} &\equiv \bar{u} \gamma_\mu u \bar{u} \gamma^\mu u, & O_{ud}^1 &\equiv \bar{u} \gamma_\mu u \bar{d} \gamma^\mu d, \\ O_{ud}^8 &\equiv \bar{u} \gamma_\mu T^A u \bar{d} \gamma^\mu T^A d, & O_{quqd}^1 &\equiv \bar{q} u \varepsilon \bar{q} d, \\ O_{quqd}^8 &\equiv \bar{q} T^A u \varepsilon \bar{q} T^A d. \end{aligned}$$

The Hermitian conjugates of scalar and tensor operators need to be added to those three lists of two- and

<sup>1</sup>See Ref. [68] for an EFT discussion of the baryon-number-violating interactions of the top quark.

four-fermion operators while the imposed Hermiticity,  $C^a_b = (C^b_a)^*$ , of vector operator coefficients ensures the reality of the effective Lagrangian.

The gauge invariance of the SM could only be imposed on fermionic gauge eigenstates. Observations, however, are related to mass eigenstates. Rotating one basis to the other is therefore required for all practical purposes. Neither the gauge-eigenstate operator coefficients, nor the unitary rotation matrices appearing in Yukawa singular-value decompositions are measurable. Physical operator coefficients and Cabibbo-Kobayashi-Maskawa (CKM) as well as Pontecorvo-Maki-Nakagawa-Sakata (PMNS) mixing matrix elements are. By removing unphysical rotation matrices, we choose the gauge eigenstates to be expressed in terms of physical eigenstates as

$$q \equiv (u_L, V_{\text{CKM}} d_L)^T, \quad u \equiv u_R, \quad d \equiv d_R, \\ l \equiv (V_{\text{PMNS}} \nu_L, e_L)^T, \quad e \equiv e_R.$$

The physical operator coefficients involving left-handed up- and down-type quarks are then related through the CKM matrix. For instance, in the  $O_{\varphi q}^1$  case,

$$\bar{q} \gamma^\mu C_{\varphi q}^1 q = \bar{u}_L \gamma^\mu C_{\varphi q}^1 u_L + \bar{d}_L \gamma^\mu [V_{\text{CKM}}^\dagger C_{\varphi q}^1 V_{\text{CKM}}] d_L. \quad (2)$$

Similarly, the coefficients of operators involving left-handed charged leptons and neutrinos are related to each other through the PMNS matrix.

Putting quark flavor indices between brackets, there are ten independent complex coefficients, for either  $a = 1$  or  $2$ , in the two-quark category:

$$C_{\varphi q}^{-(a3)} = C_{\varphi q}^{-(3a)*} \equiv C_{\varphi q}^{-(a+3)}, \\ C_{\varphi u}^{(a3)} = C_{\varphi u}^{(3a)*} \equiv C_{\varphi u}^{(a+3)}, \\ C_{u\varphi}^{(a3)}, C_{u\varphi}^{(3a)}, \\ C_{uB}^{(a3)}, C_{uB}^{(3a)}, \quad C_{uW}^{(a3)}, C_{uW}^{(3a)}, \quad C_{uG}^{(a3)}, C_{uG}^{(3a)}.$$

Without distinguishing the lepton flavors (all diagonal and nondiagonal combinations should in principle be considered independently), there are nine operators, for either  $a = 1$  or  $2$ , in the two-quark–two-lepton category:

$$C_{lq}^{-(a3)} = C_{lq}^{-(3a)*} \equiv C_{lq}^{-(a+3)}, \\ C_{lq}^{+(a3)} = C_{lq}^{+(3a)*} \equiv C_{lq}^{+(a+3)}, \\ C_{lu}^{(a3)} = C_{lu}^{(3a)*} \equiv C_{lu}^{(a+3)}, \\ C_{eq}^{(a3)} = C_{eq}^{(3a)*} \equiv C_{eq}^{(a+3)}, \\ C_{eu}^{(a3)} = C_{eu}^{(3a)*} \equiv C_{eu}^{(a+3)}, \\ C_{lequ}^{1(a3)}, C_{lequ}^{1(3a)}, \quad C_{lequ}^{3(a3)}, C_{lequ}^{3(3a)}.$$

Finally, for each allowed combination of  $a, b, c \in \{1, 2\}$ , there are 11 independent four-quark coefficients leading to top FCNC processes:

$$C_{qq}^{1(3a,bc)} = C_{qq}^{1(bc,3a)} = C_{qq}^{1(a3,cb)*}, \\ C_{qq}^{3(3a,bc)} = C_{qq}^{3(bc,3a)} = C_{qq}^{3(a3,cb)*}, \\ C_{uu}^{(3a,bc)} = C_{uu}^{(bc,3a)} = C_{uu}^{(a3,cb)*}, \\ C_{ud}^{1(3a,bc)} = C_{ud}^{1(a3,cb)*}, \quad C_{ud}^{8(3a,bc)} = C_{ud}^{8(a3,cb)*}, \\ C_{qu}^{1(3a,bc)} = C_{qu}^{1(a3,cb)*}, \quad C_{qu}^{8(3a,bc)} = C_{qu}^{8(a3,cb)*}, \\ C_{qu}^{1(bc,3a)} = C_{qu}^{1(cb,a3)*}, \quad C_{qu}^{8(bc,3a)} = C_{qu}^{8(cb,a3)*}, \\ C_{qd}^{1(3a,bc)} = C_{qd}^{1(a3,cb)*}, \quad C_{qd}^{8(3a,bc)} = C_{qd}^{8(a3,cb)*}.$$

Four-fermion operators have been overlooked in most analyses.

## B. Dimension-four and -five operators

Beside the fully gauge-invariant effective field theory that will be exploited here, different theoretical frameworks have been used in the literature to describe top-quark flavor-changing neutral currents in a model-independent way.

A very common approach is the anomalous coupling one. Its main advantage is that of being close to the Feynman rules definition and so, of easy use. It is, however, not a well-defined quantum field theory where constraints set by symmetries and radiative corrections can be taken into account systematically. Such an approach is therefore not suitable for the purpose of a global analysis at next-to-leading order in QCD.

Second, an effective-field-theory description of top-quark FCNCs in the electroweak broken phase [44,72] has been widely used. It is based on an effective Lagrangian containing dimension-four and -five operators that only satisfy Lorentz and  $SU(3)_C \times U(1)_{\text{EM}}$  gauge symmetries. This broken-phase effective Lagrangian reads

$$\mathcal{L}_{\text{eff}}^{\text{EW}} = -\frac{g_W}{2c_W} \bar{t} \gamma^\mu (v_{tq}^Z - a_{tq}^Z \gamma_5) q \quad Z_\mu \\ -\frac{g_W}{2\sqrt{2}} g_{qt} \bar{q} (g_{qt}^v + g_{qt}^a \gamma_5) t \quad h \\ -e \frac{\kappa_{tq}^\gamma}{\Lambda} \bar{t} \sigma^{\mu\nu} (f_{tq}^\gamma + i h_{tq}^\gamma \gamma_5) q \quad A_{\mu\nu} \\ -\frac{g_W}{2c_W} \frac{\kappa_{tq}^Z}{\Lambda} \bar{t} \sigma^{\mu\nu} (f_{tq}^Z + i h_{tq}^Z \gamma_5) q \quad Z_{\mu\nu} \\ -g_s \frac{\kappa_{tq}^g}{\Lambda} \bar{t} \sigma^{\mu\nu} T^A (f_{tq}^g + i h_{tq}^g \gamma_5) q \quad G_{\mu\nu}^A + \text{H.c.}, \quad (3)$$

where  $q = u$  or  $c$  and  $c_W \equiv \cos \theta_W$ . The  $\kappa_{tq}$  and  $g_{qt}$  coefficients are real and positive, while the complex

$(v_{iq}^Z, a_{iq}^Z)$ ,  $(f_{iq}, h_{iq})$  and  $(g_{qt}^v, g_{qt}^a)$  pairs satisfy  $|f_{iq}|^2 + |h_{iq}|^2 = 1$  and  $|g_{qt}^v|^2 + |g_{qt}^a|^2 = 1$ .

Without further constraint on its parameters, such an effective Lagrangian may be understood as more general than the fully gauge-invariant one. In other words, new physics is not assumed to preserve the electroweak  $SU(2)_L \times U(1)_Y$  gauge symmetry. Such a construction turns out to be way too general as it would require many coefficients to be extremely small or correlated with each other in order to reproduce measurements. This is at variance with the full  $SU(3)_C \times SU(2)_L \times U(1)_Y$  symmetry that naturally accounts for all observations made so far. For example, with full gauge invariance imposed, flavor-changing neutral currents only occur at the loop or nonrenormalizable level.

In this work, we assume that new physics preserves the full standard-model gauge invariance, at least approximately, in the energy range probed by the LHC. The Lagrangian of Eq. (3) may then be seen as a practical reparametrization of the  $SU(3)_C \times SU(2)_L \times U(1)_Y$ -invariant operators presented in the previous section. Its couplings are then tacitly understood as expressions of the fully gauge-invariant operator coefficients, the SM parameters and the scale  $\Lambda$ :

$$\begin{aligned} -\frac{g_W}{2c_W} \begin{cases} v_{iq}^Z \\ -a_{iq}^Z \end{cases} &= \frac{-e}{2s_W c_W} \frac{m_t^2}{\Lambda^2} [C_{\phi u}^{(a+3)*} \pm C_{\phi q}^{-(a+3)*}], \\ -\frac{g_W}{2\sqrt{2}} g_{qt} \begin{cases} g_{qt}^v \\ g_{qt}^a \end{cases} &= \frac{-2m_t m_t^2}{v} \frac{1}{\Lambda^2} [C_{u\phi}^{(a3)} \pm C_{u\phi}^{(3a)*}], \\ -e \frac{\kappa_{iq}^\gamma}{\Lambda} \begin{cases} f_{iq}^\gamma \\ ih_{iq}^\gamma \end{cases} &= e \frac{m_t}{\Lambda^2} [(C_{uB}^{(3a)} + C_{uW}^{(3a)}) \pm (C_{uB}^{(a3)} + C_{uW}^{(a3)*})], \\ -\frac{g_W}{2c_W} \frac{\kappa_{iq}^Z}{\Lambda} \begin{cases} f_{iq}^Z \\ ih_{iq}^Z \end{cases} &= \frac{-e}{s_W c_W} \frac{m_t}{\Lambda^2} [(s_W^2 C_{uB}^{(3a)} - c_W^2 C_{uW}^{(3a)}) \\ &\quad \pm (s_W^2 C_{uB}^{(a3)} - c_W^2 C_{uW}^{(a3)*})], \\ -g_s \frac{\kappa_{iq}^g}{\Lambda} \begin{cases} f_{iq}^g \\ ih_{iq}^g \end{cases} &= g_s \frac{m_t}{\Lambda} [C_{uG}^{(3a)} \pm C_{uG}^{(a3)*}]. \end{aligned}$$

Such a reparametrization has, however, intrinsic limitations and to some extent can lead to misconceptions. Let us list a few specific reasons.

First, the broken-phase effective Lagrangian displayed as in Eq. (3) hides the actual scaling of each contribution. It does not make explicit that FCNC operators do not appear at the renormalizable level, and therefore it does not account for the experimental lack of evidence of the corresponding effects in the first place. The hierarchies this Lagrangian displays are moreover misleading as all tree-level FCNC effects actually first appear at dimension six. The operators that are seemingly of dimension four and five actually contribute at the same order in  $1/\Lambda$ . At next-to-leading order in QCD, the  $\bar{t}\sigma^{\mu\nu}T^A qG_{\mu\nu}^A$  operators

renormalize the  $\bar{t}qh$  ones that, in the broken phase, seem to be of different dimension. On the contrary, in the fully gauge-invariant picture,  $O_{uG} \equiv \bar{q}\sigma^{\mu\nu}T^A u\tilde{\phi}G_{\mu\nu}^A$  renormalizes  $O_{u\phi} \equiv \bar{q}u\tilde{\phi}\phi^\dagger\phi$  without actually mixing dimensions. More details on the mixing between operators and their running will be provided in the next section. Note in passing that the use of a broken-phase effective Lagrangian would make the computation of NLO weak corrections intractable.

Second, some operators contributing at the same order as those appearing in Eq. (3) are not included. Namely, a  $\bar{t}\sigma^{\mu\nu}T^A qhG_{\mu\nu}^A$  operator actually contributes to  $th$  production at hadron colliders at the same order as  $\bar{t}\sigma^{\mu\nu}T^A qG_{\mu\nu}^A$  [see Fig. 1(a)]. This is trivially seen when the full gauge invariance is restored as both contributions then arise from the same dimension-six  $O_{uG}$  operator.

A complete basis should also include four-fermion operators. These are also of dimension six and can be related to two-fermion operators through the equations of motion (EOM). Such *contact* interactions could arise, for instance, in the presence of a heavy mediator coupling to two fermionic currents. They have unduly been neglected in experimental searches, Refs. [18,20] excepted. They could for example contribute to processes such as  $t \rightarrow j\ell^+\ell^-$ ,  $pp \rightarrow tj$ ,  $e^+e^- \rightarrow tj$  [Fig. 1(b)] and  $e^-p \rightarrow e^-t$ . Trying to use the equations of motion to trade them all for two-fermion operators involving more covariant derivatives is in fact vain. Those involving vector or tensor fermionic bilinears which are not flavor diagonal would not appear in any of the EOM (non-flavor-diagonal scalar bilinears, on the other hand, are present in the equations of motion for the Higgs field). In many interesting leading-order processes and in all next-to-leading-order ones, the off-shell character of the particles involved in an effective operator also precludes the use of EOM that could

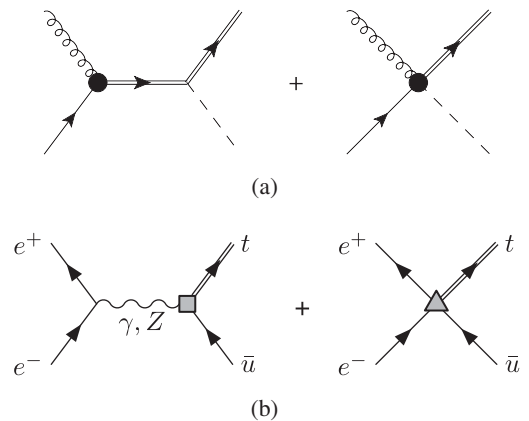


FIG. 1. The full standard-model gauge symmetry gives rise to four-point interactions, not included in the Lagrangian of Eq. (3), that contribute at the same order as three-point ones in some FCNC processes: e.g. (a) in  $ug \rightarrow th$  production (or radiative  $t \rightarrow hug$  decay), or (b) in  $e^+e^- \rightarrow t\bar{t}$  (and  $t \rightarrow ue^+e^-$ ).

render irrelevant some operators containing derivatives. In Fig. 1 some examples of processes proceeding through the exchange of off-shell particles are provided. All dominant effects of heavy new physics can therefore only be guaranteed to be modeled by an effective theory if four-fermion operators are included.

Third, by writing an effective theory in the electroweak broken phase without making explicit the expressions of the couplings in terms of the fully gauge-invariant operator coefficients, one can easily overlook correlations between operators. The  $\bar{l}\sigma^{\mu\nu}T^A q h G_{\mu\nu}^A$  and  $\bar{l}\sigma^{\mu\nu}T^A q G_{\mu\nu}^A$  interactions that derive from the same dimension-six  $O_{uG}$  operator already provided an obvious example. Such kind of full correlation due to the presence, in  $\varphi$ , of a physical Higgs particle and a vacuum expectation value occurs only above the electroweak symmetry breaking scale in processes involving an external Higgs particle or when taking loop-level contributions into account. Another type of correlation arises from the fact that left-handed down- and up-type quarks belong to a single gauge-eigenstate doublet. Operator coefficients measurable in  $B$ -meson physics (see Refs. [73,74] for recent EFT analyses exploiting the full standard-model gauge invariance) are actually related to those relevant to top-quark physics through equalities like Eq. (2) that involve  $V_{CKM}$ . The impact of  $B$ -physics constraints on top FCNC operators has for instance been studied in Refs. [75–78] with one single operator switched on at the time, though. A truly global analysis in a fully gauge-invariant EFT framework remains to be carried out. It should take advantage of all types of correlations and use several processes in which a closed set of operators contributes through different combinations. Only by doing this, is it possible to disentangle the effects coming from each of them.

### III. MIXINGS

At NLO in QCD, dimension-six operators may mix with each other. In other words, the renormalization of an operator may involve several others. Because of quantum effects, the very definition of operator coefficients actually depends on the renormalization scheme and scale. RG mixings imply that a coefficient defined at one scale is actually a combination of many others at a different scale. The information about the RG flow

$$\frac{dC_i(\mu)}{d\ln\mu} = \gamma_{ij}C_j(\mu) \quad (4)$$

is encoded in the anomalous dimension matrix  $\gamma_{ij}$  which has been computed recently for the full set of dimension-six operators [79–82] (see also Ref. [62] for a specific discussion of the anomalous dimensions of flavor-changing top-quark operators).

At a high scale, a full theory may justify specific values for operators coefficients. In particular, some of them may be negligible. However, after the RG evolution down to lower scales, mixing might lead to a significant increase of the set of operators with sizable coefficients. As an example, let us consider the Yukawa operator  $O_{u\varphi}^{(13)}$ . It can be generated from its QCD mixing only by the color-dipole operator  $O_{uG}^{(13)}$ . Over a range of scales as small as  $1 \text{ TeV} \rightarrow m_t$ , one gets

$$\left\{ \begin{array}{l} C_{uG}^{(13)}(1 \text{ TeV}) = 1, \\ C_{u\varphi}^{(13)}(1 \text{ TeV}) = 0, \end{array} \right. \longrightarrow \left\{ \begin{array}{l} C_{uG}^{(13)}(m_t) = 0.98, \\ C_{u\varphi}^{(13)}(m_t) = 0.23. \end{array} \right.$$

At the energies currently probed by experiments, it is thus unnatural to assume only one or two operator coefficients are nonzero. One should *a priori* include all operators contributing at a given order. Then, to constrain operator coefficients consistently, one should use the renormalization-group equations and evolve all available bounds to a common scale where a global analysis can then be carried out.

#### A. Renormalization patterns

The mutual renormalizations of operator coefficients entail that, at next-to-leading order (and beyond), some operators will provide counterterms regularizing UV divergent diagrams involving other ones. As an example, let us consider the  $ug \rightarrow tZ$  production process. Some representative diagrams are given in Fig. 2. The first two are leading-order amplitudes involving  $O_{uG}$  and  $O_{uW}$  operators, respectively. The third and fourth diagrams provide  $\mathcal{O}(\alpha_s)$  corrections to the second and first. The fourth contribution also requires a counterterm from  $O_{uW}$ . On the contrary, at NLO in QCD, there is no divergent diagram involving  $O_{uW}$  that would require a counterterm of  $O_{uG}$  form.

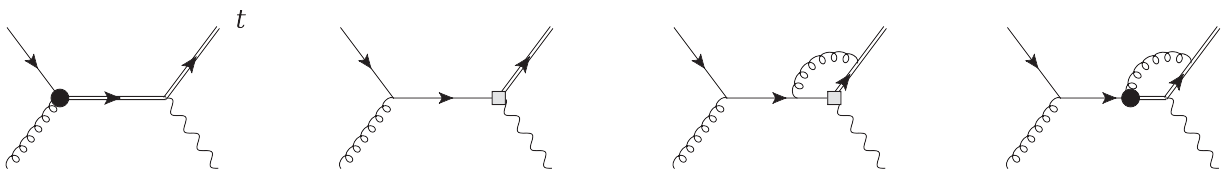


FIG. 2. Representative  $ug \rightarrow tZ$  diagrams involving  $O_{uG}$  (black dot) and  $O_{uW}$  (gray square) operators, at leading-order (first two) and next-to-leading order (last two diagrams). The UV divergence of the fourth diagram involving  $O_{uG}$  is regularized by a counterterm of  $O_{uW}$  form.

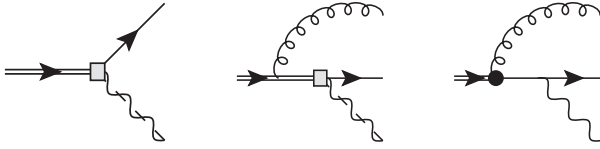


FIG. 3. Representative diagrams for  $t \rightarrow u\gamma$ ,  $qZ$ ,  $qh$  at leading and next-to-leading orders. The gray square represents a contribution from the  $O_{uW}$  weak-dipole operator, while the black dot represents a contribution from the  $O_{uG}$  color-dipole operator.

The pattern of such mutual NLO renormalizations can in principle be extracted from the RG equations of Refs. [79–82]. The full anomalous dimension matrix is, however, complicated and obtaining this information may appear nontrivial. Changing the normalization of operator coefficients so as to make their LO contributions formally of the same order renders the situation clearer. Some pieces of the RG equations for the new coefficients then formally appear of order  $\alpha_s$  and can thus be isolated. They contain the information about renormalization patterns we need.

Having taken the normalization (with  $y_t$  and  $g_{Y,W,S}$  factors) of our two-quark operators as in Ref. [62], and assuming for the moment all coefficients to have comparable magnitudes makes their LO contributions to the  $pp \rightarrow t\gamma$ ,  $tZ$  and  $th$  processes formally of the same order. Such a normalization appears natural if one considers that each boson is eventually attached to a fermionic line in the full theory from which the EFT models the low-energy effects. One then obtains a closed set of RG equations for  $C_{uq}$ ,  $C_{uB}$ ,  $C_{uW}$  and  $C_{uG}$  that are formally of order  $\alpha_s$ . The corresponding anomalous dimension matrix is given by

$$\frac{2\alpha_s}{\pi} \begin{pmatrix} -2 & 0 & 0 & -1 \\ 0 & 1/3 & 0 & 5/9 \\ 0 & 0 & 1/3 & 1/3 \\ 0 & 0 & 0 & 1/6 \end{pmatrix}.$$

Note that, due to current conservation, the coefficients of the vector  $O_{\phi q}^-$  and  $O_{\phi u}$  operators are not renormalized.

It is then transparent that  $O_{uG}$  renormalizes all other coefficients which, on the contrary, only renormalize themselves at order  $\alpha_s$ . For instance, the RG equation of  $C_{uW}^{(13)}$  at that order reads

$$\frac{dC_{uW}^{(13)}(\mu)}{d\ln\mu} = \frac{2\alpha_s}{3\pi} C_{uW}^{(13)}(\mu) + \frac{2\alpha_s}{3\pi} C_{uG}^{(13)}(\mu).$$

The first term corresponds to the running of  $C_{uW}^{(13)}$  itself, while the second one is a mixing from  $C_{uG}^{(13)}$  to  $C_{uW}^{(13)}$  formally of order  $\alpha_s$  which will cancel the UV divergences from the fourth diagram (and of diagrams not shown in Fig. 2). On the other hand,  $C_{uG}^{(13)}$  is not renormalized by  $C_{uW}^{(13)}$ :

TABLE I. Two-quark and two-quark–two-lepton operators that are renormalized by four-quark ones, at order  $\alpha_s$ .

	$O_{qq}^1, O_{qq}^3$	$O_{qu}^1$	$O_{ud}^1$	$O_{uu}$	$O_{qd}^1$
$O_{\phi q}^1$	✓	✓			✓
$O_{\phi q}^3$	✓				
$O_{\phi u}$		✓	✓	✓	
$O_{lq}^1$	✓	✓			✓
$O_{lq}^3$	✓				
$O_{lu}$		✓	✓	✓	
$O_{eq}$	✓	✓			✓
$O_{eu}$		✓	✓	✓	

$$\frac{dC_{uG}^{(13)}(\mu)}{d\ln\mu} = \frac{\alpha_s}{3\pi} C_{uG}^{(13)}(\mu)$$

at order  $\alpha_s$ .

At leading order, there is only one contribution to the  $t \rightarrow q\gamma$ ,  $qZ$  and  $qh$  decay processes: the first diagram of Fig. 3. The above procedure therefore does not apply. The second diagram is a QCD correction to the first one. Other quantum corrections involving  $O_{uG}$ , like the third diagram, are also included by analogy.

As four-fermion operators could arise from the tree-level exchange of a new heavy bosonic mediator, their coefficients could probably be chosen of new-physics order only. Examining the RG equations at order  $\alpha_s$ , it turns out that, unlike four-quark operators, two-quark–two-lepton ones do not mix between themselves (this may not be true in another basis) or with two-quark operators. The pattern of renormalization of two-quark and two-quark–two-lepton operators by four-quark ones is detailed in Table I.

#### IV. FCNC PROCESSES AT NLO IN QCD

In order to demonstrate the feasibility of an EFT treatment of top-quark FCNC processes that is NLO accurate in QCD, we discuss two specific cases. First, we consider top-quark decay processes and the—often overlooked—contributions of two-quark–two-lepton operators. Second, some NLO results merged with parton shower are presented for single top produced in association with a photon,  $Z$  or Higgs bosons.

For numerical results, here and in what follows, we use  $m_t = 172.5$  GeV,  $\alpha^{-1} = 127.9$ ,  $\alpha_s = 0.10767$ ,  $\sin^2\theta_W = 0.2337$ ,  $m_Z = 91.1876$  GeV and  $\Gamma_Z = 2.4952$  GeV. Unless otherwise specified, we set  $\Lambda = 1$  TeV.

Note dimension-six effective operators not listed here contribute, at order  $1/\Lambda^2$ , to the observables used to fix those SM parameters. As the leading contributions to the FCNC processes we are considering appear at order  $1/\Lambda^4$ , these shifts in the SM parameters only induce  $1/\Lambda^6$  corrections which can be neglected consistently.

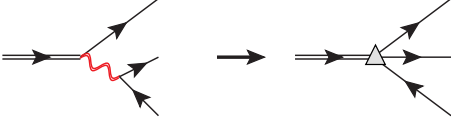


FIG. 4 (color online). The tree-level exchange of a heavy flavor-changing  $Z'$  would generate four-fermion effective operators. Such operators have been overlooked in many experimental searches.

### A. Two-quark–two-lepton operators in top decay

As stressed before, two-quark–two-lepton operators have been overlooked in top-quark FCNC searches at the LHC even though they contribute to  $pp \rightarrow t\ell^+\ell^-$ ,

$t \rightarrow j\ell^+\ell^-$  or  $e^+e^- \rightarrow tj$  processes [see Fig. 1(a)]. As they are potentially tree-level generated, for instance from the exchange of a heavy  $Z'$  (see Fig. 4), those operators may even have coefficients larger than those of two-quark operators.

Complete results at NLO in QCD for top-quark FCNC decays through two-quark and two-quark–two-lepton operators can be found in Ref. [62]. Here, we focus on the specific  $t \rightarrow j\ell^+\ell^-$  process. The two-quark operators contribute through the exchange of a (virtual) photon or  $Z$  while the two-quark–two-lepton operators lead to three-body decays. The first half of Table II presents the

TABLE II. Contributions of each FCNC operator coefficient to the  $t \rightarrow j\ell^+\ell^-$  partial width (for one single species of massless quark and charged leptons) [62]. The subscripts indicate the relative correction brought by the NLO contribution in QCD (a dash stresses the absence of leading-order contribution). Off-shell  $Z$  effects are included to all orders. In the on-peak + off-peak case, a 15 GeV cut was been applied on the invariant mass of the two leptons, to avoid the divergence of the  $t \rightarrow j\gamma^* \rightarrow j\ell^+\ell^-$  contribution. In the *on-peak* case,  $m_{\ell\ell} \in [78, 102]$  GeV is required.

$\Gamma_{t \rightarrow j\ell^+\ell^-}^{\text{on-peak+off-peak}} / 10^{-5} \text{ GeV} \times (\Lambda/1 \text{ TeV})^4$	
$= \text{Re} \begin{pmatrix} C_{lq}^{-(a+3)} \\ C_{eq}^{(a+3)} \\ C_{\phi q}^{-(a+3)} \\ C_{uB}^{(a3)} \\ C_{uW}^{(a3)} \\ C_{uG}^{(a3)} \end{pmatrix} \dagger \begin{pmatrix} +0.29 & 0 & -0.035 & -0.23i & -0.19 & -0.11i & -0.33 & +0.38i & +0.026 & -0.0025i \\ -8\% & & -12\% & -8\% & -7\% & -8\% & -7\% & -8\% & & \\ +0.29 & +0.028 & +0.028 & +0.18i & -0.25 & +0.087i & -0.14 & -0.30i & +0.00064 & +0.023i \\ -8\% & -8\% & -12\% & -8\% & -7\% & -8\% & -7\% & -8\% & & \\ & +1.9 & +1.8 & -0.016i & -6.2 & -0.016i & +0.29 & +0.22i & & \\ -8\% & -8\% & -8\% & -8\% & -8\% & -8\% & -8\% & -8\% & & \\ & +0.91 & +0.91 & -3.6 & -0.049i & +0.14 & +0.12i & & & \\ -9\% & -9\% & -9\% & -9\% & -9\% & -9\% & -9\% & -9\% & & \\ & & & +7.6 & -0.61 & -0.55i & & & & \\ & & & -9\% & & & +0.0068 & & & \end{pmatrix} \begin{pmatrix} C_{lq}^{-(a+3)} \\ C_{eq}^{(a+3)} \\ C_{\phi q}^{-(a+3)} \\ C_{uB}^{(a3)} \\ C_{uW}^{(a3)} \\ C_{uG}^{(a3)} \end{pmatrix}$	$+ \text{Re} \begin{pmatrix} C_{lu}^{(a+3)} \\ C_{eu}^{(a+3)} \\ C_{\phi u}^{(a+3)} \\ C_{uB}^{(3a)*} \\ C_{uW}^{(3a)*} \\ C_{uG}^{(3a)*} \end{pmatrix} \dagger \begin{pmatrix} +0.29 & 0 & -0.035 & -0.23i & -0.19 & -0.11i & -0.33 & +0.38i & +0.0068 & +0.021i \\ -8\% & & -12\% & -8\% & -7\% & -8\% & -7\% & -8\% & & \\ +0.29 & +0.028 & +0.028 & +0.18i & -0.25 & +0.087i & -0.14 & -0.30i & +0.016 & +0.0043i \\ -8\% & -8\% & -12\% & -8\% & -7\% & -8\% & -7\% & -8\% & & \\ & +1.9 & +1.8 & -0.016i & -6.2 & -0.016i & -0.18 & -0.092i & & \\ -8\% & -8\% & -8\% & -8\% & -8\% & -8\% & -8\% & -8\% & & \\ & +0.91 & +0.91 & -3.6 & -0.049i & -0.13 & -0.096i & & & \\ -9\% & -9\% & -9\% & -9\% & -9\% & -9\% & -9\% & -9\% & & \\ & & & +7.6 & +0.31 & +0.19i & & & & \\ & & & -9\% & & & +0.0053 & & & \end{pmatrix} \begin{pmatrix} C_{lu}^{(a+3)} \\ C_{eu}^{(a+3)} \\ C_{\phi u}^{(a+3)} \\ C_{uB}^{(3a)*} \\ C_{uW}^{(3a)*} \\ C_{uG}^{(3a)*} \end{pmatrix}$
$+0.082( C_{lequ}^{1(13)} ^2 +  C_{lequ}^{1(31)} ^2) + 3.5( C_{lequ}^{3(13)} ^2 +  C_{lequ}^{3(31)} ^2)$	
$\Gamma_{t \rightarrow j\ell^+\ell^-}^{\text{on-peak}} / 10^{-5} \text{ GeV} \times (\Lambda/1 \text{ TeV})^4$	
$= \text{Re} \begin{pmatrix} C_{lq}^{-(a+3)} \\ C_{eq}^{(a+3)} \\ C_{\phi q}^{-(a+3)} \\ C_{uB}^{(a3)} \\ C_{uW}^{(a3)} \\ C_{uG}^{(a3)} \end{pmatrix} \dagger \begin{pmatrix} +0.069 & 0 & -0.02 & -0.2i & -0.053 & -0.1i & -0.052 & +0.34i & +0.014 & -0.013i \\ -9\% & & +6\% & -9\% & -5\% & -8\% & -16\% & -8\% & & \\ +0.069 & +0.017 & +0.017 & +0.18i & -0.053 & +0.09i & -0.054 & -0.3i & -0.007 & +0.017i \\ -9\% & +6\% & +6\% & -9\% & -10\% & -8\% & +0\% & -8\% & & \\ & +1.7 & +1.7 & -0.0095i & +1.7 & -0.0095i & -5.7 & -0.0095i & +0.27 & +0.2i \\ -9\% & -9\% & -8\% & -8\% & -8\% & -8\% & -8\% & -8\% & & \\ & +0.64 & +0.64 & -3.9 & -0.029i & +0.16 & +0.14i & & & \\ -9\% & -9\% & -9\% & -9\% & -9\% & -9\% & -9\% & -9\% & & \\ & & & +6.6 & -0.53 & -0.47i & & & & \\ & & & -9\% & & & +0.002 & & & \end{pmatrix} \begin{pmatrix} C_{lq}^{-(a+3)} \\ C_{eq}^{(a+3)} \\ C_{\phi q}^{-(a+3)} \\ C_{uB}^{(a3)} \\ C_{uW}^{(a3)} \\ C_{uG}^{(a3)} \end{pmatrix}$	$+ \text{Re} \begin{pmatrix} C_{lu}^{(a+3)} \\ C_{eu}^{(a+3)} \\ C_{\phi u}^{(a+3)} \\ C_{uB}^{(3a)*} \\ C_{uW}^{(3a)*} \\ C_{uG}^{(3a)*} \end{pmatrix} \dagger \begin{pmatrix} +0.069 & 0 & -0.02 & -0.2i & -0.053 & -0.1i & -0.052 & +0.34i & -0.002 & +0.013i \\ -9\% & & +6\% & -9\% & -5\% & -8\% & -16\% & -8\% & & \\ +0.069 & +0.017 & +0.017 & +0.18i & -0.053 & +0.09i & -0.054 & -0.3i & +0.0067 & -0.006i \\ -9\% & +6\% & +6\% & -9\% & -10\% & -8\% & +0\% & -8\% & & \\ & +1.7 & +1.7 & -0.0095i & +1.7 & -0.0095i & -5.7 & -0.0095i & -0.17 & -0.09i \\ -9\% & -9\% & -8\% & -8\% & -8\% & -8\% & -8\% & -8\% & & \\ & +0.64 & +0.64 & -3.9 & -0.029i & -0.098 & -0.068i & & & \\ -9\% & -9\% & -9\% & -9\% & -9\% & -9\% & -9\% & -9\% & & \\ & & & +6.6 & +0.31 & +0.21i & & & & \\ & & & -9\% & & & +0.00066 & & & \end{pmatrix} \begin{pmatrix} C_{lu}^{(a+3)} \\ C_{eu}^{(a+3)} \\ C_{\phi u}^{(a+3)} \\ C_{uB}^{(3a)*} \\ C_{uW}^{(3a)*} \\ C_{uG}^{(3a)*} \end{pmatrix}$
$+0.02( C_{lequ}^{1(13)} ^2 +  C_{lequ}^{1(31)} ^2) + 0.81( C_{lequ}^{3(13)} ^2 +  C_{lequ}^{3(31)} ^2)$	

numerical contributions of each operator coefficient to the partial decay width. As light-fermion masses have been neglected, operators involving light fermions of different chiralities do not interfere. Only the contributions of  $O_{uG}$  (where a photon or  $Z$  is emitted from the quark line) differ between the left- and right-handed light quark cases.

Remarkably, for operator coefficients of equal magnitude, the  $O_{lequ}^3$  two-quark–two-lepton operators contribute in proportions comparable to two-quark ones. The lepton invariant mass distributions of two-quark operator contributions are however strongly peaked around  $m_Z$  (see Fig. 5). Current searches for top-quark FCNC decays to a light jet and a lepton pair actually focus on lepton invariant mass windows close to the  $Z$ -boson mass (e.g.,  $m_{\ell\ell} \in [78, 102]$  GeV) and interpret the obtained result as limits on  $t \rightarrow jZ$ , without taking into account two-quark–two-lepton operator contributions. However, even in this on- $Z$ -peak window, the second part of Table II shows some residual sensitivity to two-quark–two-lepton operators,  $O_{lequ}^3$  especially. Neglecting interferences and considering only operators  $O_{\bar{q}q}^-$ ,  $O_{uW}$  and  $O_{lequ}^3$  for the sake of illustration, Table II gives

$$\begin{aligned} \Gamma_{t \rightarrow ue^+e^-}^{\text{on-peak}} / 10^{-5} \text{ GeV} \times (\Lambda/1 \text{ TeV})^4 \\ = 1.7 |C_{\bar{q}q}^{-(1+3)}|^2 + 6.6 |C_{uW}^{(13)}|^2 + 0.81 |C_{lequ}^{3(13)}|^2. \end{aligned} \quad (5)$$

On the other hand, in the off-peak region of the spectrum,  $m_{\ell\ell} \in [15, 78] \cup [102, \infty]$  GeV, one has

$$\begin{aligned} \Gamma_{t \rightarrow ue^+e^-}^{\text{off-peak}} / 10^{-5} \text{ GeV} \times (\Lambda/1 \text{ TeV})^4 \\ = 0.2 |C_{\bar{q}q}^{-(1+3)}|^2 + 1.0 |C_{uW}^{(13)}|^2 + 2.7 |C_{lequ}^{3(13)}|^2. \end{aligned} \quad (6)$$

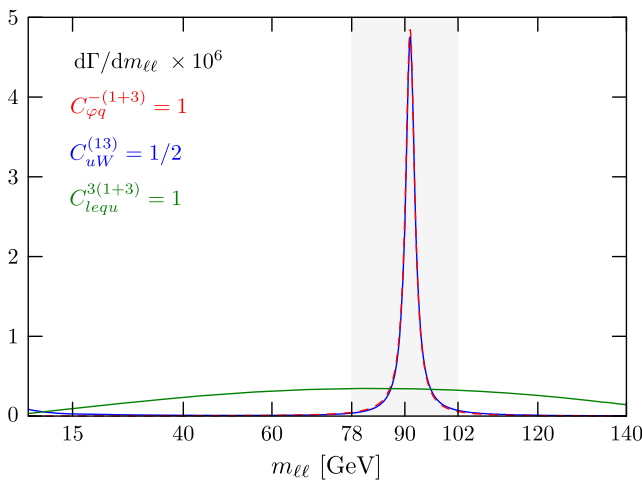


FIG. 5 (color online). Invariant mass distribution of lepton pair in  $t \rightarrow j\ell^+\ell^-$ . Contributions from two-quark  $O_{\bar{q}q}^-$  and  $O_{uW}$  as well as two-quark–two-lepton  $O_{lequ}^3$  operators are compared.

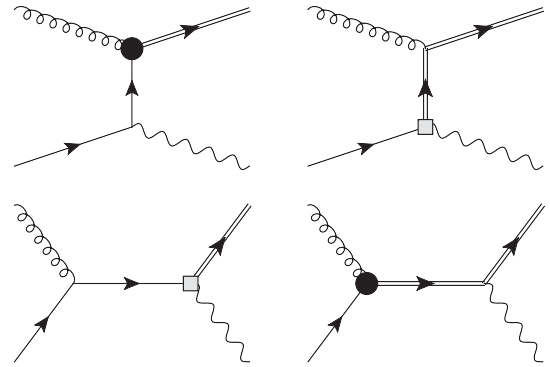


FIG. 6. Tree-level diagrams for  $pp \rightarrow t\gamma$  and  $pp \rightarrow tZ$ .

By distinguishing both regions, one therefore gets a means of constraining separately two-quark and two-quark–two-lepton operators. Moreover, were a signal to be observed, its proportion in each of those ranges of lepton invariant masses would bring information about its nature. As the off-peak region contains less Drell-Yan background, a better sensitivity may actually be obtained on two-quark–two-lepton operator coefficients.

Similarly, one may use angular distributions to disentangle the contributions of vector, scalar and tensor operators, as done in Ref. [28]. In Ref. [62], the  $Z$  helicity fractions were also computed at NLO in QCD as functions of operator coefficients. Taking into account differential decay rates should therefore allow us to disentangle all types of operators. Since identifying final-state up- and charm-quark jets can only be done with a limited efficiency, one should rely on production processes and take benefit of the widely different parton distribution functions of  $u$ 's and  $c$ 's to discriminate between both contributions.

## B. Single-top production

Single-top production associated with a neutral gauge boson,  $\gamma$ ,  $Z$ , or the scalar boson  $h$  can bring useful information on top-quark FCNC [42,44,51–57]. As illustrated in Figs. 6 and 7,  $O_{uG}$  already contributes at leading order to  $pp \rightarrow t\gamma$  or  $pp \rightarrow tZ$  and  $pp \rightarrow th$ . Following the general strategy outlined in Ref. [83], all two-quark

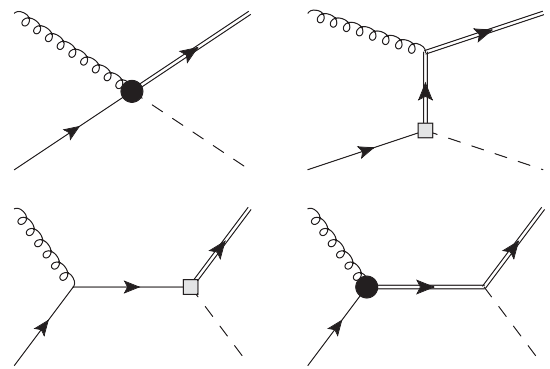


FIG. 7. Tree-level diagrams for  $pp \rightarrow th$ .



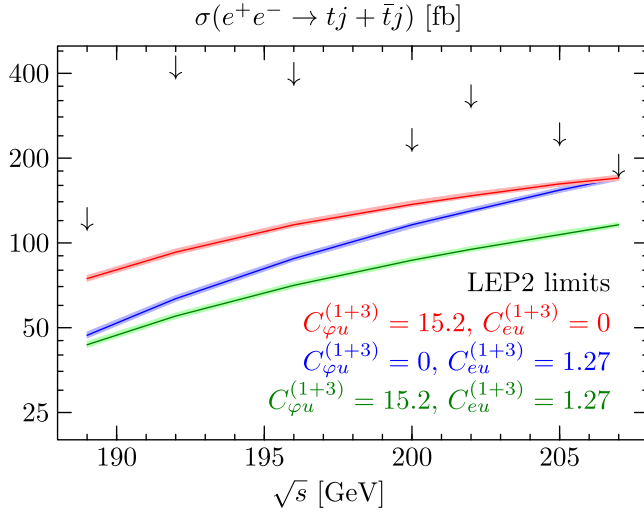


FIG. 8 (color online). Cross section [fb] for  $e^+e^- \rightarrow tj + \bar{t}j$  for three illustrative choices of parameters at NLO accuracy in QCD (lines); 95% C.L. limits (arrows) set by a combination ALEPH, DELPHI, L3 and OPAL results [15]. The uncertainty bands ( $+2.2\%$  at  $\sqrt{s} = 207$  GeV) are obtained by running  $\alpha_s$  from  $m_t/2$  to  $2m_t$  as the anomalous dimensions of vector operators vanish.

operators have been implemented in the FEYNRULES/MADGRAPH5\_AMC@NLO simulation chain [84–86] which permits automated NLO computations in QCD, including matching to parton shower. The details of this implementation are discussed elsewhere [87].

A  $m_{\ell\ell}$ -dependent reweighing can also be used to obtain, from two-quark operator results, the NLO-accurate contributions of vector (and scalar) two-quark–two-lepton operators. Such operators have not yet been implemented in MADGRAPH5\_AMC@NLO. Figure 8 compares  $e^+e^- \rightarrow tj + \bar{t}j$  production cross sections through a two-quark and a two-quark–two-lepton operator, as well as through their interference. The bounds deriving from a combination of

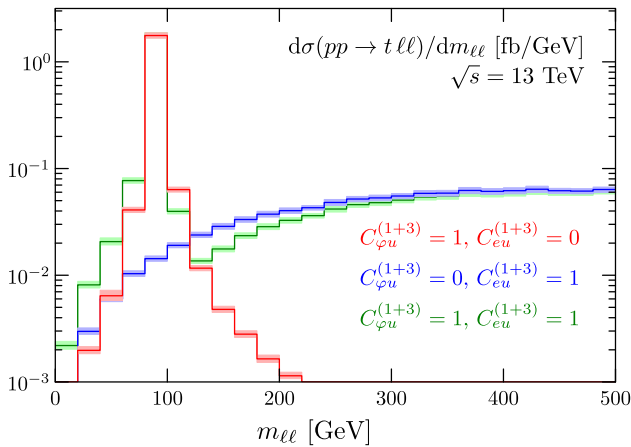


FIG. 9 (color online). NLO lepton invariant mass distribution in  $pp \rightarrow t\ell\bar{\ell}$ , from the two-quark operator  $O_{\varphi u}$  only (red), from the two-quark–two-lepton operators  $O_{e u}$  (blue) and from their interference (green).

LEP2 results [15] are also shown. In Fig. 9 the contributions of the same two operators,  $O_{\varphi u}$  and  $O_{e u}$ , to  $pp \rightarrow t\ell^+\ell^-$  at  $\sqrt{s} = 13$  TeV are shown. In those figures, the uncertainty bands are obtained from factorization and renormalization scale variations between  $m_t/2$  and  $2m_t$ .

## V. A FIRST GLOBAL ANALYSIS

In this section we illustrate the feasibility of a global approach to top-quark FCNC interactions. For the sake of illustration and simplicity, we only consider the most constraining observables. This suffices to set significant bounds on all two-quark operators listed previously as well as on a subset of the two-quark–two-lepton ones. Four-fermion operators featuring two leptons of different generations or a pair of taus would remain unconstrained due to the absence of experimental searches while those with two muons are only loosely bound due to the lack of off- $Z$ -peak constraint in  $t \rightarrow j\ell^+\ell^-$  searches. LEP2 data, however, effectively constrain operators containing an electron pair. We will neglect the contributions of four-quark operators to considered observables. They are suppressed by an imposed jet veto in  $pp \rightarrow t$  and only appear at NLO in QCD in the other processes we take into account.

Currently, for either  $j = u$  or  $c$ , the most constraining 95% C.L. bounds on the top-quark branching ratios are<sup>23</sup>

$$\text{Br}(t \rightarrow je^+e^-) + \text{Br}(t \rightarrow j\mu^+\mu^-) \lesssim 0.0017 \quad [33],$$

$$\text{Br}(t \rightarrow j\gamma) < 3.2\% \quad [26],$$

$$\text{Br}(t \rightarrow j\gamma\gamma) < 0.0016\% \quad [35].$$

(Top and antitop branching fractions are assumed identical by the experimental collaborations.) The first limit is actually applicable for lepton invariant masses close to  $m_Z$ :  $m_{\ell\ell} \in [78, 102]$  GeV. The CMS Collaboration actually interprets it as a bound on  $\text{Br}(t \rightarrow jZ)$  even though four-fermion operator contributions cannot in general be neglected. Similarly, the third limit is obtained for  $m_{\gamma\gamma} \in [120, 130]$  GeV and interpreted as a bound on  $\text{Br}(t \rightarrow ch)$  while the contributions of  $uth$  and  $u(c)t\gamma$  interactions should in principle also be taken into account. Furthermore, a limit on the single-top production cross section [8]

$$\sigma(pp \rightarrow t) + \sigma(pp \rightarrow \bar{t}) < 2.5 \text{ pb} \quad \text{at } \sqrt{s} = 8 \text{ TeV}$$

<sup>2</sup>Those two figures are obtained using  $\text{Br}(Z \rightarrow \ell^+\ell^-) = 3.37\%$  [88] as well as the CMS limit on  $\text{Br}(t \rightarrow jZ) < 0.05\%$  which combines the  $e^+e^-$  and  $\mu^+\mu^-$  channels. They may therefore be slightly underestimated and do not account for the difference in efficiency of these two channels.

<sup>3</sup>The limit on  $\text{Br}(t \rightarrow ch) < 0.69\%$  and the assumed  $\text{Br}(h \rightarrow \gamma\gamma) = 0.23\%$  both quoted in Table IV have been used.

is converted by the ATLAS Collaboration into the  $\text{Br}(t \rightarrow ug) < 0.0031\%$  and  $\text{Br}(t \rightarrow cg) < 0.016\%$  bounds on top-quark FCNC branching fractions when a  $tug$  or a  $tcg$  vertex are respectively assumed to provide the only contributions to the above cross section. Similarly, the

$$\begin{aligned} & \sigma(ug \rightarrow t\gamma) + \sigma(ug \rightarrow \bar{t}\gamma) \\ & + 0.778[\sigma(cg \rightarrow t\gamma) + \sigma(cg \rightarrow \bar{t}\gamma)] \\ & < 0.0670 \text{ pb} \quad \text{at } \sqrt{s_{pp}} = 8 \text{ TeV} \end{aligned}$$

bound obtained by the CMS Collaboration [13]<sup>4</sup> for  $p_{T\gamma} > 30 \text{ GeV}$  is translated into the  $\text{Br}(t \rightarrow u\gamma) < 0.0108\%$  and  $\text{Br}(t \rightarrow c\gamma) < 0.132\%$  limits by taking into account either  $u\gamma$  or  $c\gamma$  contributions only (the  $ut\gamma$  and  $ct\gamma$  contributions are notably assumed vanishing). Finally, a LEP2 combination [15] implies

$$\sigma(e^+e^- \rightarrow tj + \bar{t}j) < 176 \text{ fb} \quad \text{at } \sqrt{s} = 207 \text{ GeV}$$

for  $m_t = 172.5 \text{ GeV}$ .

### A. $t \rightarrow j\ell^+\ell^-$

Let us first consider the top decay to a pair of charged leptons and a jet. It is mainly sensitive to operators inducing a  $t \rightarrow jZ$  decay. At leading order, the rate for this process can be expressed as a sum of four squared terms corresponding to final states of different polarizations ( $q_L Z_0$ ,  $q_R Z_0$ ,  $q_L Z_-$  and  $q_R Z_+$ ):

$$\begin{aligned} \Gamma_{t \rightarrow jZ} &= \frac{\alpha m_t^5 (1-x^2)^2}{8\Lambda^4 s_W^2 c_W^2} \\ & \times \sum_{a=1,2} \left\{ \left| \frac{1}{2x} C_{\varphi q}^{-(a+3)} + 2x \left( s_W^2 C_{uB}^{(a3)} - c_W^2 C_{uW}^{(a3)} \right) \right|^2 \right. \\ & + \left| \frac{1}{2x} C_{\varphi u}^{(a+3)} + 2x \left( s_W^2 C_{uB}^{(3a)*} - c_W^2 C_{uW}^{(3a)*} \right) \right|^2 \\ & + 2 \left| \frac{1}{2} C_{\varphi q}^{-(a+3)} + 2 \left( s_W^2 C_{uB}^{(a3)} - c_W^2 C_{uW}^{(a3)} \right) \right|^2 \\ & \left. + 2 \left| \frac{1}{2} C_{\varphi u}^{(a+3)} + 2 \left( s_W^2 C_{uB}^{(3a)*} - c_W^2 C_{uW}^{(3a)*} \right) \right|^2 \right\}, \end{aligned}$$

where  $x \equiv m_Z/m_t$ ,  $s_W \equiv \sin \theta_W$  and  $c_W \equiv \cos \theta_W$ . Therefore,  $t \rightarrow j\ell^+\ell^-$  in the on- $Z$ -peak region dominantly constrains four linear combinations of  $C_{\varphi q}^{-(a+3)}$ ,  $C_{\varphi u}^{(a+3)}$ ,  $C_{uB}^{(a3)}$ ,  $C_{uW}^{(a3)}$  and  $C_{uB}^{(3a)}$ ,  $C_{uW}^{(3a)}$  for both  $a = 1$  and  $2$ .

Numerical results that are NLO accurate in QCD, include the full  $\Gamma_Z$  dependence and all the two-quark–two-lepton

operators have been collected in Table II. At that order, a dependence on the  $O_{uG}$  operator coefficients is generated. It has, however, little overall effect given the tight constraints of  $C_{uG}$  that arise from  $pp \rightarrow t, \bar{t}$  searches.

### B. $pp \rightarrow t, \bar{t}$

The most sensitive of the single-top production limits constrains the  $C_{uG}$  coefficients alone, provided the four-quark operator contributions in the experimental acceptance are neglected. Using the NLO result

$$\Gamma_{t \rightarrow jj} = B\Gamma_t \left( \frac{1 \text{ TeV}}{\Lambda} \right)^4 \sum_{a=1,2} \left( |C_{uG}^{(a3)}|^2 + |C_{uG}^{(3a)}|^2 \right),$$

with  $B \equiv 0.0186$  and a fixed value for the top width  $\Gamma_t = 1.32 \text{ GeV}$ , we recast the interpretation made in Ref. [8] to obtain the bound on the operator coefficient combination actually probed in  $pp \rightarrow t + \bar{t}$ :

$$\begin{aligned} & \frac{1}{B_u} (|C_{uG}^{(13)}|^2 + |C_{uG}^{(31)}|^2) + \frac{1}{B_c} (|C_{uG}^{(23)}|^2 + |C_{uG}^{(32)}|^2) \\ & < \frac{1}{B} \left( \frac{\Lambda}{1 \text{ TeV}} \right)^4, \end{aligned}$$

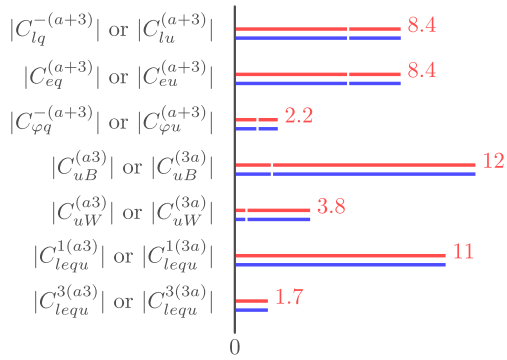
where  $\text{Br}(t \rightarrow ug) < 0.0031\% \equiv B_u$  and  $\text{Br}(t \rightarrow cg) < 0.016\% \equiv B_c$  are the limits set assuming one single contribution from either  $a=1$  or  $a=2$ . Fixing  $\Lambda = 1 \text{ TeV}$ , the following—strong—constraints are obtained on the coefficient moduli:

$$|C_{uG}^{(a3)}| \text{ or } |C_{uG}^{(3a)}| \begin{cases} \color{red} 0.041 \\ \color{blue} 0.093 \\ 0 \end{cases}$$

where the red allowed range applies to up-quark operator coefficients ( $a = 1$ ) and blue ranges to charm-quark ones ( $a = 2$ ).

Actually, at this stage, all operator coefficients but the  $C_{u\varphi}$  ones are already constrained, sometimes poorly though. Most notably, the  $t \rightarrow j\ell^+\ell^-$  observable is primarily sensitive to the  $s_W^2 O_{uB} - c_W^2 O_{uW}$  linear combinations that contain the tensorial  $Z$  interactions, while  $O_{uB} + O_{uW}$  contains the photon ones. The absence of experimental bound outside the on- $Z$ -peak region for  $m_{\ell\ell}$  also renders the two-quark–two-lepton operators very loosely constrained. Quantitatively with the two observables just described, the limits that arise on the moduli of the operator coefficients are

<sup>4</sup>This expression is obtained from the bounds on the NLO cross sections times  $W$  leptonic branching fraction [we took  $\text{Br}(W \rightarrow \nu_l) = 3 \times 10.80\%$  [88]] provided by the CMS Collaboration.



where the white marks indicate the bounds that would have been obtained out of our global picture, by assuming that all coefficients but the constrained one vanish. Among those limits, only the ones applying to  $|C_{\varphi q}^-|$  or  $|C_{\varphi u}|$  will not improve much in what follows.

### C. $t \rightarrow j\gamma$ and $pp \rightarrow t\gamma, \bar{t}\gamma$

Breaking the approximate degeneracy between the  $C_{uB}$  and  $C_{uW}$  coefficients present in  $t \rightarrow j\ell^+\ell^-$  can be achieved through top-quark FCNC processes involving a photon. The CDF Collaboration still currently sets the best limit on the top decay to a photon and a jet:  $\text{Br}(t \rightarrow j\gamma) < 3.2\%$  [26]. The corresponding leading-order decay rate writes

$$\Gamma_{t \rightarrow j\gamma} = \frac{\alpha m_t^5}{\Lambda^4} \sum_{a=1,2} \left( |C_{uB}^{(a3)} + C_{uW}^{(a3)}|^2 + |C_{uB}^{(3a)} + C_{uW}^{(3a)}|^2 \right).$$

At order  $\mathcal{O}(\alpha_s)$ , a cut on the photon energy and jet-photon separation is required to avoid the soft-collinear divergence. For  $(E_{\gamma,j}, \mathbf{p}_{\gamma,j})$  the quadrimomenta of the photon and quark jet in the top rest frame, we take

$$1 - \mathbf{p}_\gamma \cdot \mathbf{p}_j / E_\gamma E_j > 0.2, \quad E_\gamma > 20 \text{ GeV}.$$

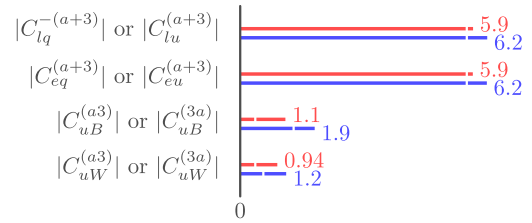
With these cuts the CDF constraint reads

$$\begin{aligned} & \sum_{a=1,2} \{ |0.71C_{uB}^{(a3)} + 0.71C_{uW}^{(a3)} - 0.036C_{uG}^{(a3)}|^2 \\ & \quad \times |0.71C_{uB}^{(3a)} + 0.71C_{uW}^{(3a)} - 0.036C_{uG}^{(3a)}|^2 \} \\ & < 19.6 \frac{3.2\%}{\text{Br}_{t \rightarrow j\gamma}^{\text{exp}}} \frac{\Gamma_t}{1.32 \text{ GeV}} \left( \frac{\Lambda}{1 \text{ TeV}} \right)^4. \end{aligned} \quad (7)$$

A much stronger constraint on  $C_{uB} + C_{uW}$  is actually obtained by considering the bound set in Ref. [13] on single-top production in association with a photon of transverse momentum  $p_{T\gamma} > 30 \text{ GeV}$ . Taking into account the relative efficiency obtained by CMS for up-gluon and charm-gluon initial states and NLO results in QCD for  $\sigma(pp \rightarrow t\gamma + \bar{t}\gamma)$  at  $\sqrt{s} = 8 \text{ TeV}$  obtained with the implementation of Ref. [87] in AMC@NLO [86] we get

$$\begin{aligned} & \begin{pmatrix} C_{uB}^{(13)} \\ C_{uW}^{(13)} \\ C_{uG}^{(13)} \end{pmatrix}^\dagger \begin{pmatrix} 0.46 & 0.93 & 0.2 \\ & 0.46 & 0.2 \\ & & 1.9 \end{pmatrix} \begin{pmatrix} C_{uB}^{(13)} \\ C_{uW}^{(13)} \\ C_{uG}^{(13)} \end{pmatrix} + (13) \leftrightarrow (31) \\ & + 0.78 \begin{pmatrix} C_{uB}^{(23)} \\ C_{uW}^{(23)} \\ C_{uG}^{(23)} \end{pmatrix}^\dagger \begin{pmatrix} 0.047 & 0.095 & 0.017 \\ & 0.047 & 0.017 \\ & & 0.33 \end{pmatrix} \begin{pmatrix} C_{uB}^{(23)} \\ C_{uW}^{(23)} \\ C_{uG}^{(23)} \end{pmatrix} \\ & + (23) \leftrightarrow (32) \\ & < 0.067 (\Lambda/1 \text{ TeV})^4. \end{aligned}$$

With this observable taken into account, the limits on  $C_{uB}$  and  $C_{uW}$  improve dramatically. Indirectly, the bounds on two-quark–two-lepton operators that interfere with those in  $t \rightarrow j\ell^+\ell^-$  also improve slightly:



The complementarity of  $t \rightarrow j\ell^+\ell^-$  and  $pp \rightarrow t\gamma, \bar{t}\gamma$  observables is illustrated in Fig. 10.

### D. $e^+e^- \rightarrow tj, \bar{t}j$

Without an off-Z-peak constraint on  $t \rightarrow j\ell^+\ell^-$ , one cannot do better for the two-quark–two-lepton operators involving muons. However, the limit set at LEP on

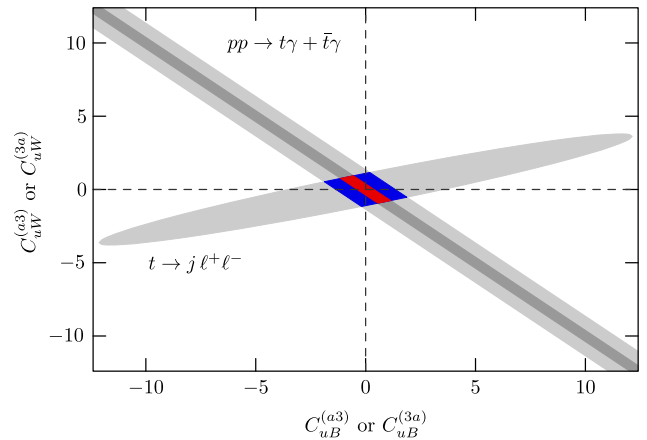


FIG. 10 (color online). Complementarity of the  $t \rightarrow j\ell^+\ell^-$  and  $pp \rightarrow t\gamma, \bar{t}\gamma$  limits in the  $C_{uB} - C_{uW}$  plane. The  $C_{uG}$  coefficients are constrained to satisfy the bounds set by the  $pp \rightarrow t, \bar{t}$  searches. The dark gray and red allowed regions apply for  $a = 1$  while the blue intersection shows the constraint for  $a = 2$ . The same limits apply to either the real or the imaginary parts of the operator coefficients.

TABLE III. NLO expression for the  $e^+e^- \rightarrow tj$  cross section in fb, including full  $\Gamma_Z$  dependence, for either  $a = 1$  or 2 (light quark and electron masses are neglected). For  $e^+e^- \rightarrow \bar{t}j$  the two complex matrices should be conjugated. As the experimental constraint is set on  $tj$  plus  $\bar{t}j$  production, the imaginary prefactors provided here at leading order only have no effect on our limits. Identical bounds therefore apply to the real and imaginary parts of each operator coefficient. The  $C_{lequ}^{1,3}$  prefactors are obtained fully analytically (see the Appendix) while the other ones, from the AMC@NLO implementation of Ref. [87] either directly, for two-fermion operators, or after reweighing, for four-fermion ones.

$$\begin{aligned}
& \sigma_{e^+e^- \rightarrow tj}^{\sqrt{s}=207 \text{ GeV}} [\text{fb}] \times (\Lambda/1 \text{ TeV})^4 \\
& = \text{Re} \begin{pmatrix} C_{lq}^{-(a+3)*} \\ C_{eq}^{(a+3)*} \\ C_{\varphi q}^{-(1+3)*} \\ C_{uB}^{(a3)*} \\ C_{uW}^{(a3)*} \\ C_{uG}^{(a3)*} \end{pmatrix}^\dagger \begin{pmatrix} +52_{+24\%} & 0 & +6.5 - 0.035i_{+25\%} & -9 - 0.036i_{+24\%} & -38 + 0.12i_{+24\%} & +1_{-} \\ +52_{+24\%} & +52_{+24\%} & -5.7 + 0.03i_{+25\%} & -22 + 0.032i_{+24\%} & +3.8 - 0.1i_{+25\%} & +0.04_{-} \\ & & +0.37_{+25\%} & +0.63 - 0.00064i_{+24\%} & -2.6 - 0.00064i_{+25\%} & +0.061_{-} \\ & & & +2.7_{+25\%} & +2.5 - 0.003i_{+23\%} & -0.1_{-} \\ & & & & +7.3_{+25\%} & -0.37_{-} \\ & & & & & +1.6 \times 10^{-5}_{-} \end{pmatrix} \begin{pmatrix} C_{lq}^{-(a+3)*} \\ C_{eq}^{(a+3)*} \\ C_{\varphi q}^{-(a+3)*} \\ C_{uB}^{(a3)*} \\ C_{uW}^{(a3)*} \\ C_{uG}^{(a3)*} \end{pmatrix} \\
& + \text{Re} \begin{pmatrix} C_{lu}^{(a+3)*} \\ C_{eu}^{(a+3)*} \\ C_{qu}^{(a+3)*} \\ C_{uB}^{(3a)} \\ C_{uW}^{(3a)} \\ C_{uG}^{(3a)} \end{pmatrix}^\dagger \begin{pmatrix} +52_{+24\%} & 0 & +6.5 - 0.035i_{+25\%} & -9 - 0.036i_{+24\%} & -38 + 0.12i_{+24\%} & +1_{-} \\ +52_{+24\%} & +52_{+24\%} & -5.7 + 0.03i_{+25\%} & -22 + 0.032i_{+24\%} & +3.8 - 0.1i_{+25\%} & +0.71_{-} \\ & & +0.37_{+25\%} & +0.63 - 0.00064i_{+24\%} & -2.6 - 0.00064i_{+25\%} & +0.024_{-} \\ & & & +2.7_{+24\%} & +2.5 - 0.003i_{+23\%} & -0.24_{-} \\ & & & & +7.3_{+25\%} & -0.35_{-} \\ & & & & & +1.6 \times 10^{-5}_{-} \end{pmatrix} \begin{pmatrix} C_{lu}^{(a+3)*} \\ C_{eu}^{(a+3)*} \\ C_{qu}^{(1+3)*} \\ C_{uB}^{(3a)} \\ C_{uW}^{(3a)} \\ C_{uG}^{(3a)} \end{pmatrix} \\
& + 33_{+42\%} (|C_{lequ}^{1(a3)}|^2 + |C_{lequ}^{1(3a)}|^2) + 370_{+26\%} (|C_{lequ}^{3(a3)}|^2 + |C_{lequ}^{3(3a)}|^2)
\end{aligned}$$

$e^+e^- \rightarrow tj + \bar{t}j$  [15] gives a powerful handle on the two-quark–two-lepton operators involving electrons. The next-to-leading-order expression for  $\sigma(e^+e^- \rightarrow tj)$  at  $\sqrt{s} = 207$  GeV is provided in Table III. As can be seen from Fig. 8, the bound set at this center-of-mass energy is the most constraining one. We do not attempt a combination of the bounds set at different center-of-mass energies that could only be naive given the lack of published statistical information.

The complementarity of the LEP limit with the  $t \rightarrow je^+e^-$  one for constraining simultaneously two- and four-fermion operators is illustrated in Fig. 11.

### E. $t \rightarrow j\gamma\gamma$

Finally, the  $C_{u\varphi}$  coefficients can be bound using the  $t \rightarrow j\gamma\gamma$  search presented in Ref. [35]. As mentioned before, the interpretation the CMS Collaboration overlooks a dependence in the flavor-changing  $t\gamma q$  couplings. Imposing  $m_{\gamma\gamma} \in [120, 130]$  GeV and  $m_{\gamma j} > 10$  GeV with  $m_h = 125$  GeV and  $\text{Br}(h \rightarrow \gamma\gamma) = 0.23\%$ , we get

$$\begin{aligned}
\Gamma_{t \rightarrow j\gamma\gamma}^{\text{on-}h\text{-peak}} &= 1.09 \times 10^{-6} \text{ GeV} \quad (1 \text{ TeV}/\Lambda)^4 \\
&\times \sum_{a=1,2} \{ |C_{u\varphi}^{(a3)}|^2 + |C_{u\varphi}^{(3a)}|^2 \\
&+ 0.37 (|C_{uB}^{(a3)} + C_{uW}^{(a3)}|^2 + |C_{uB}^{(3a)} + C_{uW}^{(3a)}|^2) \}
\end{aligned}$$

at leading order, with the interference between the  $C_{uB} + C_{uW}$  and the  $C_{u\varphi}$  contributions neglected. However, given the bounds set previously on  $C_{uB} + C_{uW}$  and the relatively mild constraint on  $t \rightarrow j\gamma\gamma$ , those  $t\gamma q$  contributions have no

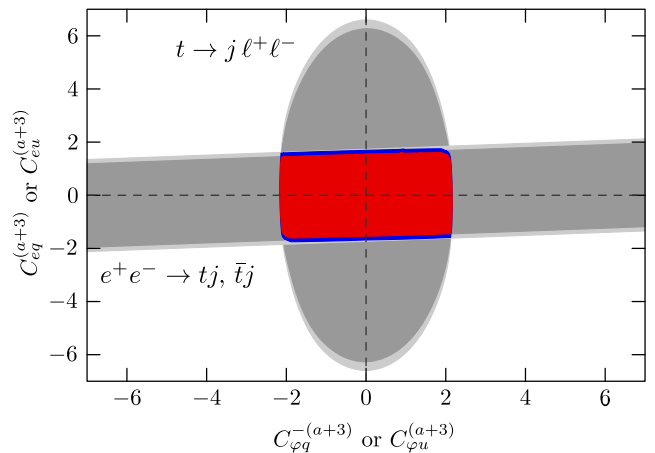


FIG. 11 (color online). Complementarity of the  $e^+e^- \rightarrow tj + \bar{t}j$  and  $t \rightarrow je^+e^-$  limits for constraining two- and four-fermion operators. The operator coefficients not shown in this plane are constrained to satisfy the bound of Fig. 12. The dark gray and red allowed regions apply for  $a = 1$  while the light gray and blue ones for  $a = 2$ . The same limits apply to either the real or the imaginary parts of the operator coefficients.

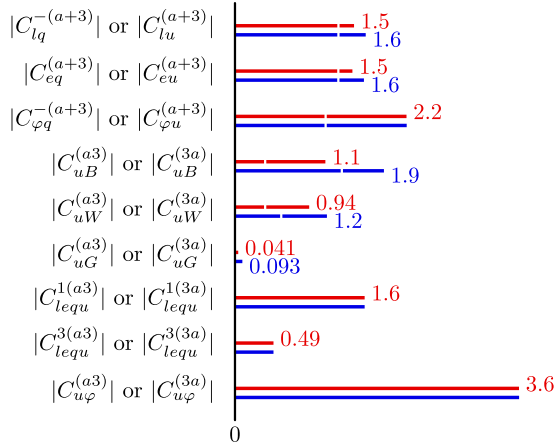


FIG. 12 (color online). The 95% C.L. limits on the moduli of operator coefficients for  $\Lambda = 1$  TeV, as deriving from current bounds on  $t \rightarrow j\ell^+\ell^-$ ,  $t \rightarrow j\gamma\gamma$ ,  $pp \rightarrow t + \bar{t}$ ,  $pp \rightarrow t\gamma + \bar{t}\gamma$  and  $e^+e^- \rightarrow tj + \bar{t}j$ . Two-quark–two-lepton operators containing an electron pair are shown; for the one containing a muon pair we refer to the figures in Secs. V B and V C. The red allowed regions apply for  $a = 1$  and the blue ones for  $a = 2$ . A white mark indicates the bound that would have been obtained by fixing all coefficients to zero but the one constrained, instead of performing a global analysis.

significant impact on the global limits we set. We therefore consider the following NLO [89] constraint instead:

$$\begin{aligned} & \sum_{a=1,2} \{ |0.9997 C_{u\varphi}^{(a3)} - 0.0243 C_{uG}^{(a3)}|^2 \\ & + |0.9997 C_{u\varphi}^{(3a)} - 0.0243 C_{uG}^{(3a)}|^2 \} \\ & < 12.8 \frac{0.69\% \cdot 0.23\%}{\text{Br}_{t \rightarrow jh}^{\text{exp}} \text{Br}_{h \rightarrow \gamma\gamma}} \frac{\Gamma_t}{1.32 \text{ GeV}} \left( \frac{\Lambda}{1 \text{ TeV}} \right)^4. \end{aligned}$$

Unfortunately, a statistical combination of the 95% C.L. bounds derived in this section is not possible with the published information. We can only require those constraints to be simultaneously satisfied. The results of this procedure are shown in Fig. 12.

## VI. CONCLUSIONS

A fully gauge-invariant effective field theory allows the consistent, global and accurate interpretation of new-physics searches in terms of well-defined theoretical parameters. Our global analysis at NLO in QCD of the most constraining limits on top-quark FCNC operators provides a proof of principle of feasibility of this program.

In particular, we have stressed the importance of considering simultaneously all contributions arising at dimension six in the standard-model effective theory, four-fermion operators included. Separating on-Z-peak and off-Z-peak lepton invariant mass regions in  $t \rightarrow j\ell^+\ell^-$  searches would allow us to better constrain

two-quark–two-lepton operators, especially the ones involving a muon pair. Distinguishing the lepton channels would permit us to bound accurately different operators. In general, efficiencies for each contribution and fiducial limits should be made public. Angular distributions—helicity fractions notably—would provide additional separation power between operators of different Lorentz structures. The effort devoted to the searches of top-quark FCNC production processes should be pursued further as they probe higher-energy scales than decays. In particular, an update of the limit on  $pp \rightarrow t\ell^-\ell^+$  and a search for  $pp \rightarrow th$  would probably improve significantly the constraints presented here. Ultimately, the publication of the statistical information from which the limits derive would allow for a more appropriate combination of the constraints coming from different observables.

In this work, we have made the first steps towards a global approach to the determination of the top-quark couplings in the context of an effective field theory by considering the case of FCNC interactions at NLO in QCD. The same approach can be extended to flavor-conserving and charged-current interactions. The impact of indirect constraints arising from  $B$  mesons, electroweak or Higgs data could (and should) also be considered. In this respect the effective field theory provides a unique framework where all information coming from different measurements and observables can be consistently, accurately and precisely combined to set bounds on new physics.

## ACKNOWLEDGMENTS

We would like to thank Mojtaba Najafabadi, Reza Goldouzian and Andrea Giammanco for details about the analysis of Ref. [13]. This work has been performed in the framework of the ERC Grant No. 291377 “LHCTheory” and of the FP7 Marie Curie Initial Training Network MCnetITN (Grant No. PITN-GA-2012-315877). C.Z. has been supported by the IISN “Fundamental interactions” convention 4.4517.08, and by U.S. Department of Energy under Grant No. DE-AC02-98CH10886. G.D. is a Research Fellow of the FNRS, Belgium, and of the Belgian American Education Foundation, USA.

## APPENDIX: NLO CORRECTIONS TO $e^+e^- \rightarrow tj$

NLO cross sections for  $e^+e^- \rightarrow tj$  can be written as

$$\sigma^{\text{NLO}} = \sigma^{\text{LO}} \left[ 1 + \frac{\alpha_s(\mu)}{\pi} \delta(x, \mu) \right]$$

where  $\mu$  is the renormalization scale, and  $x = m_t/\sqrt{s}$ . The quantum corrections  $\delta$  depend on the Lorentz structure of the quark current. We obtain, for a vector current,

$$\delta(x, \mu) = \frac{1}{3(1-x^2)(2+x^2)} \left[ 6 - 9x^2 - 5x^4 + \frac{4x^2}{1-x^2} (5x^4 - 4x^2 - 5) \log(x) \right. \\ \left. - 2(1-x^2)(5x^2 + 4) \log(1-x^2) + 8(1-x^2)(2+x^2)(\log(x) \log(1-x^2) + \text{Li}_2(x^2)) \right],$$

for a scalar current,

$$\delta(x, \mu) = \frac{1}{3} \left[ -6 \log\left(\frac{s}{\mu^2}\right) + 17 + 8 \frac{x^2(x^2-2)}{(1-x^2)} \log(x) + 2(2x^2-5) \log(1-x^2) + 8 \log(x) \log(1-x^2) + 8 \text{Li}_2(x^2) \right],$$

and, finally, for a tensor current,

$$\delta(x, \mu) = \frac{1}{9(1-x^2)(1+2x^2)} \left[ 6(1-x^2)(1+2x^2) \left( \log\left(\frac{s}{\mu^2}\right) + 4 \log(x) \log(1-x^2) + 4 \text{Li}_2(x^2) \right) \right. \\ \left. + 24 \frac{5x^6 - 7x^4 + x^2}{1-x^2} \log(x) - 6(1-x^2)(1+8x^2) \log(1-x^2) - 32x^4 + 13x^2 + 7 \right].$$

- 
- [1] B. Mele, S. Petrarca, and A. Soddu, A new evaluation of the  $t \rightarrow cH$  decay width in the standard model, *Phys. Lett. B* **435**, 401 (1998).
- [2] G. Eilam, J. Hewett, and A. Soni, Rare decays of the top quark in the standard and two Higgs doublet models, *Phys. Rev. D* **44**, 1473 (1991).
- [3] J. Aguilar-Saavedra and B. Nobre, Rare top decays  $t \rightarrow c\gamma$ ,  $t \rightarrow cg$  and CKM unitarity, *Phys. Lett. B* **553**, 251 (2003).
- [4] G. Aad *et al.* (ATLAS Collaboration), Observation of a new particle in the search for the Standard Model Higgs boson with the ATLAS detector at the LHC, *Phys. Lett. B* **716**, 1 (2012).
- [5] S. Chatrchyan *et al.* (CMS Collaboration), Observation of a new boson at a mass of 125 GeV with the CMS experiment at the LHC, *Phys. Lett. B* **716**, 30 (2012).
- [6] K. A. Olive *et al.* (Particle Data Group), Review of particle physics, *Chin. Phys. C* **38**, 090001 (2014).
- [7] T. Aaltonen *et al.* (CDF Collaboration), Search for Top-Quark Production via Flavor-Changing Neutral Currents in  $W + 1$  Jet Events at CDF, *Phys. Rev. Lett.* **102**, 151801 (2009).
- [8] ATLAS Collaboration, Report No. ATLAS-CONF-2013-063, 2013.
- [9] G. Aad *et al.* (ATLAS Collaboration), Search for FCNC single top-quark production at  $\sqrt{s} = 7$  TeV with the ATLAS detector, *Phys. Lett. B* **712**, 351 (2012).
- [10] V.M. Abazov *et al.* (D0 Collaboration), Search for flavor changing neutral currents via quark-gluon couplings in single top quark production using  $2.3 \text{ fb}^{-1}$  of  $p\bar{p}$  collisions, *Phys. Lett. B* **693**, 81 (2010).
- [11] V. Abazov *et al.* (D0 Collaboration), Search for Production of Single Top Quarks via  $tcg$  and  $tug$  Flavor-Changing-Neutral-Current couplings, *Phys. Rev. Lett.* **99**, 191802 (2007).
- [12] CMS Collaboration, Report No. CMS-PAS-TOP-14-007, 2014.
- [13] CMS Collaboration, Report No. CMS-PAS-TOP-14-003, 2014.
- [14] CMS Collaboration, Report No. CMS-PAS-TOP-12-021, 2013.
- [15] LEP Exotica Working Group, Report No. LEP-Exotica-WG-2001-01, 2001.
- [16] G. Abbiendi *et al.* (OPAL Collaboration), Search for single top quark production at LEP-2, *Phys. Lett. B* **521**, 181 (2001).
- [17] A. Heister *et al.* (ALEPH Collaboration), Search for single top production in  $e^+e^-$  collisions at  $\sqrt{s}$  up to 209 GeV, *Phys. Lett. B* **543**, 173 (2002).
- [18] P. Achard *et al.* (L3 Collaboration), Search for single top production at LEP, *Phys. Lett. B* **549**, 290 (2002).
- [19] J. Abdallah *et al.* (DELPHI Collaboration), Search for single top production via FCNC at LEP at  $\sqrt{s} = 189$  GeV to 208 GeV, *Phys. Lett. B* **590**, 21 (2004).
- [20] J. Abdallah *et al.* (DELPHI Collaboration), Search for single top quark production via contact interactions at LEP2, *Eur. Phys. J. C* **71**, 1555 (2011).
- [21] H. Abramowicz *et al.* (ZEUS Collaboration), Search for single-top production in  $ep$  collisions at HERA, *Phys. Lett. B* **708**, 27 (2012).
- [22] S. Chekanov *et al.* (ZEUS Collaboration), Search for single top production in  $ep$  collisions at HERA, *Phys. Lett. B* **559**, 153 (2003).

- [23] (H1 Collaboration), Search for single top production in  $e^\pm p$  collisions at HERA, <https://www-h1.desy.de/psfiles/confpap/EPS2001/H1prelim-01-163.ps>.
- [24] F. Aaron *et al.* (H1 Collaboration), Search for single top quark production at HERA, *Phys. Lett. B* **678**, 450 (2009).
- [25] A. Aktas *et al.* (H1 Collaboration), Search for single top quark production in  $ep$  collisions at HERA, *Eur. Phys. J. C* **33**, 9 (2004).
- [26] F. Abe *et al.* (CDF Collaboration), Search for flavor-changing neutral current decays of the top quark in  $p\bar{p}$  collisions at  $\sqrt{s} = 1.8$  TeV, *Phys. Rev. Lett.* **80**, 2525 (1998).
- [27] T. Aaltonen *et al.* (CDF Collaboration), Search for the Flavor Changing Neutral Current Decay  $t \rightarrow Zq$  in  $p\bar{p}$  Collisions at  $\sqrt{s} = 1.96$  TeV, *Phys. Rev. Lett.* **101**, 192002 (2008).
- [28] T. Aaltonen *et al.* (CDF Collaboration), Search for the neutral current top quark decay  $t \rightarrow Zc$  using ratio of Z-boson + 4 jets to W-boson + 4 jets production, *Phys. Rev. D* **80**, 052001 (2009).
- [29] V.M. Abazov *et al.* (D0 Collaboration), Search for flavor changing neutral currents in decays of top quarks, *Phys. Lett. B* **701**, 313 (2011).
- [30] G. Aad *et al.* (ATLAS Collaboration), A search for flavour changing neutral currents in top-quark decays in  $pp$  collision data collected with the ATLAS detector at  $\sqrt{s} = 7$  TeV, *J. High Energy Phys.* **09** (2012) 139.
- [31] ATLAS Collaboration, Report No. ATLAS-CONF-2011-154, 2011.
- [32] ATLAS Collaboration, Report No. ATLAS-CONF-2011-061, 2011.
- [33] S. Chatrchyan *et al.* (CMS Collaboration), Search for Flavor-Changing Neutral Currents in Top-Quark Decays  $t \rightarrow Zq$  in  $pp$  Collisions at  $\sqrt{s} = 8$  TeV, *Phys. Rev. Lett.* **112**, 171802 (2014).
- [34] S. Chatrchyan *et al.* (CMS Collaboration), Search for flavor changing neutral currents in top quark decays in  $pp$  collisions at 7 TeV, *Phys. Lett. B* **718**, 1252 (2013).
- [35] CMS Collaboration, Report No. CMS-PAS-HIG-13-034, 2014.
- [36] ATLAS Collaboration, Report No. ATLAS-CONF-2013-081, 2013.
- [37] G. Aad *et al.* (ATLAS Collaboration), Search for top quark decays  $t \rightarrow qH$  with  $H \rightarrow \gamma\gamma$  using the ATLAS detector, *J. High Energy Phys.* **06** (2014) 008.
- [38] S. Weinberg, Phenomenological Lagrangians, *Physica (Amsterdam)* **96A**, 327 (1979).
- [39] S. Weinberg, Effective gauge theories, *Phys. Lett.* **91B**, 51 (1980).
- [40] H. Georgi, Effective field theory, *Annu. Rev. Nucl. Part. Sci.* **43**, 209 (1993).
- [41] S. Bar-Shalom and J. Wudka, Flavor changing single top quark production channels at  $e^+e^-$  colliders in the effective Lagrangian description, *Phys. Rev. D* **60**, 094016 (1999).
- [42] J. Aguilar-Saavedra and G. Branco, Probing top flavor changing neutral scalar couplings at the CERN LHC, *Phys. Lett. B* **495**, 347 (2000).
- [43] A. Cordero-Cid, M. Perez, G. Tavares-Velasco, and J. Toscano, Effective Lagrangian approach to Higgs-mediated FCNC top quark decays, *Phys. Rev. D* **70**, 074003 (2004).
- [44] J. Aguilar-Saavedra, Top flavor-changing neutral interactions: Theoretical expectations and experimental detection, *Acta Phys. Pol. B* **35**, 2695 (2004).
- [45] P. Ferreira, O. Oliveira, and R. Santos, Flavor changing strong interaction effects on top quark physics at the LHC, *Phys. Rev. D* **73**, 034011 (2006).
- [46] P. Ferreira and R. Santos, Strong flavor changing effective operator contributions to single top quark production, *Phys. Rev. D* **73**, 054025 (2006).
- [47] P. Ferreira and R. Santos, Contributions from dimension six strong flavor changing operators to  $t$  anti- $t$ ,  $t$  plus gauge boson, and  $t$  plus Higgs boson production at the LHC, *Phys. Rev. D* **74**, 014006 (2006).
- [48] R. B. Guedes, Flavour changing at colliders in the effective theory approach, [arXiv:0811.2136](https://arxiv.org/abs/0811.2136).
- [49] P. Ferreira, R. Guedes, and R. Santos, Combined effects of strong and electroweak FCNC effective operators in top quark physics at the CERN LHC, *Phys. Rev. D* **77**, 114008 (2008).
- [50] R. A. Coimbra, P. M. Ferreira, R. B. Guedes, O. Oliveira, A. Onofre, R. Santos, and M. Won, Dimension six flavor changing neutral current operators and top-quark production at the LHC, *Phys. Rev. D* **79**, 014006 (2009).
- [51] C. Kao, H.-Y. Cheng, W.-S. Hou, and J. Sayre, Top decays with flavor changing neutral Higgs interactions at the LHC, *Phys. Lett. B* **716**, 225 (2012).
- [52] D. Atwood, S. K. Gupta, and A. Soni, Constraining the flavor changing Higgs couplings to the top-quark at the LHC, *J. High Energy Phys.* **10** (2014) 57.
- [53] J.-L. Agram, J. Andrea, E. Conte, B. Fuks, D. Gelé, and P. Lansonneur, Probing top anomalous couplings at the LHC with trilepton signatures in the single top mode, *Phys. Lett. B* **725**, 123 (2013).
- [54] S. Khatibi and M. M. Najafabadi, Probing the anomalous FCNC interactions in top-Higgs final state and charge ratio approach, *Phys. Rev. D* **89**, 054011 (2014).
- [55] A. Greljo, J. F. Kamenik, and J. Kopp, Disentangling flavor violation in the top-Higgs sector at the LHC, *J. High Energy Phys.* **07** (2014) 046.
- [56] H. Khanpour, S. Khatibi, M. K. Yanehsari, and M. M. Najafabadi, Single top quark production as a probe of anomalous  $tq\gamma$  and  $tqZ$  couplings at the FCC-ee, [arXiv:1408.2090](https://arxiv.org/abs/1408.2090).
- [57] N. Kidonakis and A. Belyaev, FCNC top quark production via anomalous  $tqV$  couplings beyond leading order, *J. High Energy Phys.* **12** (2003) 004.
- [58] J. J. Zhang, C. S. Li, J. Gao, H. Zhang, Z. Li, C.-P. Yuan, and T.-C. Yuan, Next-to-leading-order QCD corrections to the top-quark decay via model-independent flavor-changing neutral-current couplings, *Phys. Rev. Lett.* **102**, 072001 (2009).
- [59] J. Drobnak, S. Fajfer, and J. F. Kamenik, Flavor changing neutral coupling mediated radiative top quark decays at next-to-leading order in QCD, *Phys. Rev. Lett.* **104**, 252001 (2010).
- [60] J. Drobnak, S. Fajfer, and J. F. Kamenik, QCD corrections to flavor changing neutral coupling mediated rare top quark decays, *Phys. Rev. D* **82**, 073016 (2010).
- [61] J. J. Zhang, C. S. Li, J. Gao, H. X. Zhu, C.-P. Yuan, and T.-C. Yuan, Next-to-leading order QCD corrections to the

- top quark decay via the flavor-changing neutral-current operators with mixing effects, *Phys. Rev. D* **82**, 073005 (2010).
- [62] C. Zhang, Effective field theory approach to top-quark decay at next-to-leading order in QCD, *Phys. Rev. D* **90**, 014008 (2014).
- [63] J. J. Liu, C. S. Li, L. L. Yang, and L. G. Jin, Next-to-leading order QCD corrections to the direct top quark production via model-independent FCNC couplings at hadron colliders, *Phys. Rev. D* **72**, 074018 (2005).
- [64] J. Gao, C. S. Li, J. J. Zhang, and H. X. Zhu, Next-to-leading order QCD corrections to the single top quark production via model-independent  $t$ - $q$ - $g$  flavor-changing neutral-current couplings at hadron colliders, *Phys. Rev. D* **80**, 114017 (2009).
- [65] Y. Zhang, B. H. Li, C. S. Li, J. Gao, and H. X. Zhu, Next-to-leading order QCD corrections to the top quark associated with  $\gamma$  production via model-independent flavor-changing neutral-current couplings at hadron colliders, *Phys. Rev. D* **83**, 094003 (2011).
- [66] B. H. Li, Y. Zhang, C. S. Li, J. Gao, and H. X. Zhu, Next-to-leading order QCD corrections to  $tZ$  associated production via the flavor-changing neutral-current couplings at hadron colliders, *Phys. Rev. D* **83**, 114049 (2011).
- [67] Y. Wang, F. P. Huang, C. S. Li, B. H. Li, D. Y. Shao, and J. Wang, Constraints on flavor-changing neutral-current  $Htq$  couplings from the signal of  $tH$  associated production with QCD next-to-leading order accuracy at the LHC, *Phys. Rev. D* **86**, 094014 (2012).
- [68] Z. Dong, G. Durieux, J.-M. Gerard, T. Han, and F. Maltoni, Baryon number violation at the LHC: The top option, *Phys. Rev. D* **85**, 016006 (2012).
- [69] W. Buchmuller and D. Wyler, Effective Lagrangian analysis of new interactions and flavor conservation, *Nucl. Phys.* **B268**, 621 (1986).
- [70] B. Grzadkowski, M. Iskrzynski, M. Misiak, and J. Rosiek, Dimension-six terms in the Standard Model Lagrangian, *J. High Energy Phys.* **10** (2010) 085.
- [71] J. Aguilar-Saavedra, Effective four-fermion operators in top physics: A roadmap, *Nucl. Phys.* **B843**, 638 (2011).
- [72] M. Beneke, I. Efthymiopoulos, M. L. Mangano, J. Womersley, A. Ahmadov *et al.*, Top quark physics, [arXiv:hep-ph/0003033](https://arxiv.org/abs/hep-ph/0003033).
- [73] R. Alonso, B. Grinstein, and J. Martin Camalich,  $SU(2) \times U(1)$  Gauge invariance and the shape of new physics in rare  $B$  decays, *Phys. Rev. Lett.* **113**, 241802 (2014).
- [74] A. J. Buras, J. Girrbach-Noe, C. Niehoff, and D. M. Straub,  $B \rightarrow K^{(*)}\nu\bar{\nu}$  decays in the Standard Model and beyond, *J. High Energy Phys.* **02** (2015) 184.
- [75] P. J. Fox, Z. Ligeti, M. Papucci, G. Perez, and M. D. Schwartz, Deciphering top flavor violation at the LHC with  $B$  factories, *Phys. Rev. D* **78**, 054008 (2008).
- [76] X.-Q. Li, Y.-D. Yang, and X.-B. Yuan, Anomalous  $tq\gamma$  coupling effects in exclusive radiative  $B$ -meson decays, *J. High Energy Phys.* **08** (2011) 075.
- [77] X.-Q. Li, Y.-D. Yang, and X.-B. Yuan, Anomalous  $tqZ$  coupling effects in rare  $B$ - and  $K$ -meson decays, *J. High Energy Phys.* **03** (2012) 018.
- [78] H. Gong, Y.-D. Yang, and X.-B. Yuan, Constraints on anomalous  $tcZ$  coupling from  $\bar{B} \rightarrow \bar{K}^*\mu^+\mu^-$  and  $B_s \rightarrow \mu^+\mu^-$  decays, *J. High Energy Phys.* **05** (2013) 062.
- [79] E. E. Jenkins, A. V. Manohar, and M. Trott, Renormalization group evolution of the Standard Model dimension six operators I: Formalism and lambda dependence, *J. High Energy Phys.* **10** (2013) 087.
- [80] E. E. Jenkins, A. V. Manohar, and M. Trott, Renormalization group evolution of the Standard Model dimension six operators II: Yukawa dependence, *J. High Energy Phys.* **01** (2014) 035.
- [81] R. Alonso, E. E. Jenkins, A. V. Manohar, and M. Trott, Renormalization group evolution of the Standard Model dimension six operators III: Gauge coupling dependence and phenomenology, *J. High Energy Phys.* **04** (2014) 159.
- [82] R. Alonso, H.-M. Chang, E. E. Jenkins, A. V. Manohar, and B. Shotwell, Renormalization group evolution of dimension-six baryon number violating operators, *Phys. Lett. B* **734**, 302 (2014).
- [83] N. Christensen, P. de Aquino, C. Degrande, C. Duhr, B. Fuks, M. Herquet, F. Maltoni, and S. Schumann, A comprehensive approach to new physics simulations, *Eur. Phys. J. C* **71**, 1541 (2011).
- [84] A. Alloul, N. D. Christensen, C. Degrande, C. Duhr, and B. Fuks, FeynRules 2.0 - A complete toolbox for tree-level phenomenology, *Comput. Phys. Commun.* **185**, 2250 (2014).
- [85] C. Degrande, C. Duhr, B. Fuks, D. Grellscheid, O. Mattelaer, and T. Reiter, UFO - The universal FeynRules output, *Comput. Phys. Commun.* **183**, 1201 (2012).
- [86] J. Alwall, R. Frederix, S. Frixione, V. Hirschi, F. Maltoni, O. Mattelaer, H.-S. Shao, T. Stelzer, P. Torrielli, and M. Zaro, The automated computation of tree-level and next-to-leading order differential cross sections, and their matching to parton shower simulations, *J. High Energy Phys.* **07** (2014) 079.
- [87] C. Degrande, F. Maltoni, J. Wang, and C. Zhang, Automatic computations at next-to-leading order in QCD for top-quark flavor-changing neutral processes, *Phys. Rev. D* **91**, 034024 (2015).
- [88] J. Beringer *et al.* (Particle Data Group), Review of particle physics (RPP), *Phys. Rev. D* **86**, 010001 (2012).
- [89] C. Zhang and F. Maltoni, Top-quark decay into Higgs boson and a light quark at next-to-leading order in QCD, *Phys. Rev. D* **88**, 054005 (2013).